hexagon:2611.01136v1

THE CACERES DIVISOR CROSS-ENERGY: ZEROS ON THE CRITICAL LINE, AN ARITHMETIC FOURIER QUASICRYSTAL AND A QUANTUM GRAPH OF THE PRIMES

PEDRO CACERES

Abstract. Cut the Dirichlet series of the Riemann zeta function by the divisors of an integer m instead of by size, and symmetrize it under $s \leftrightarrow 1-s$ at the scale $M = m\,\mathrm{rad}(m)$. The result, the Caceres divisor cross-energy $D_m(s) = M^{s-1}\sigma_{-s}(m) + M^{-s}\sigma_{s-1}(m)$, has all its zeros on the critical line for every m: the Euler product factorizes the cut, and each prime, taken alone, is stable because its coefficients grow by the ratio $\sqrt{p}$. We show that this simple object is completely solvable and has a rich structure. Its zeros obey an exact Riemann–von Mangoldt formula $N_m(T) = \lfloor T\log M/\pi + \frac{1}{2} + S_m(T)\rfloor$, where S_m is the argument of the Euler product of ζ over the primes of m; the phase is a sum of Poisson kernels and the gaps are rigid. The zero set is a Fourier quasicrystal: its zero measure is given in closed form by Blaschke products in the variables p^{iT}, its Bragg spectrum lies on the group generated by the $\log p$, and an exact extinction rule (axes and orthants $j \geq n(K+1)$) decides which peaks vanish; the peak at $\log M$ is always extinct. The supremum of S_m is a sum of local terms, so each lattice cell of length $\pi/\log M$ contains exactly one zero when $\sum_{p\mid m} H(p,a_p) < \frac{\pi}{2}$ and not when the sum exceeds $\frac{\pi}{2}$; $m = 12$ sits exactly on the boundary, through $\arctan\sqrt{2} + \arcsin(1/\sqrt{3}) = \frac{\pi}{2}$, and the interlacing integers have density ≈ 0.824. For multiplicative coefficients on the divisors we classify when all zeros stay on the line: exactly when no local Euler factor vanishes to the right of it, a local Lee–Yang condition with no compensation between primes. The zeros are the spectrum of an explicit quantum graph with $2K_p$ bonds of length $\log p$ for each $p \mid m$; in the language of statistical mechanics D_m is the self-dual symmetrization of the partition function of a finite primon gas, and its free energy develops a corner at $\beta = \frac{1}{2}$. Finally the zeros form a Riesz basis of exponentials on $(-\log M, \log M)$, an arithmetic sampling set, and $m = 2$ sits exactly on Kadec's $\frac{1}{4}$ threshold. The paper also contains the genealogy of the zeros of the reflected cross-energy cut by size, with the Davenport–Heilbronn and Epstein controls, and the bridge from divisors to sizes, which is the convergence of partial Euler products in the strip.

Contents

1. Introduction 2
1.1. Context 2
1.2. Results and their status 2
1.3. Related work by the author 3
2. The Hermite–Biehler form of C_2^{FR} 4
3. Genealogy of the zeros 4
4. Coefficient families 6
5. The translation law 6
6. The Epstein control 6

Date: November 2026.

2020 *Mathematics Subject Classification.* Primary 11M26, 42A75; Secondary 11M41, 11N64, 30C15, 30D15, 81Q35, 82B26, 94A20.

Key words and phrases. divisor function, Fourier quasicrystal, crystalline measure, Lee–Yang zeros, quantum graph, primon gas, Riesz basis of exponentials, sampling, reflected cross-energy, Hermite–Biehler class, Eneström–Kakeya theorem, Epstein zeta function, Davenport–Heilbronn function, partial Euler products, prime zeta function, zeros of exponential sums.

7. The Caceres divisor cross-energy 7
8. The zeros on the line: exact counting and rigidity 14
9. The zero set is a Fourier quasicrystal 15
10. The exact supremum of the counting error and interlacing 16
11. Classification: a local Lee–Yang condition 18
12. A quantum graph of the primes, and a primon gas 20
12.1. The operator 20
12.2. A primon gas 20
13. Sampling: the zeros as a Riesz basis of exponentials 21
14. The bridge from divisors to sizes 22
15. The λ-ladder 23
16. The harmonic-function criterion revisited 23
17. The cross-energy of the primes 25
18. What C_2^{FR} can decide analytically 25
18.1. Factorization 25
18.2. A Turán-type criterion 26
18.3. The nodal count of C_2 26
18.4. The weighted trapezoid form 26
19. Discussion 27
20. Open notes 28
Data and code 28
Use of AI assistance 28
References 28

1. Introduction

1.1. **Context.** The reflected cross-energy of [CE32] is

$$C_2^{\mathrm{FR}}(N,s) = X_N(s)X_N(1-s) - X_{N-1}(s)X_{N-1}(1-s) - \frac{1}{N} = N^{-s}X_{N-1}(1-s) + N^{s-1}X_{N-1}(s), \tag{1}$$

with $X_N(s) = \sum_{k\le N} k^{-s}$. Its closed form is

$$C_2^{\mathrm{FR}}(N,s) = \frac{1}{\lambda_s} - \frac{1}{N} - \frac{1}{12N^2} + \frac{2-3\lambda_s}{240N^4} + \zeta(s)N^{s-1} + \zeta(1-s)N^{-s} + O\big((1+|s|)^5 N^{-6}\big), \tag{2}$$

$\lambda_s = s(1-s)$. The closed form shows that the arithmetic content of C_2^{FR} is the pair $(\zeta(s), \zeta(1-s))$, that C_2^{FR} collapses to $\frac{1}{\lambda_\rho} - \frac{1}{N} + \cdots$ at every zero, and that at a zero on the line it changes sign once, at $N^* = \lambda_\rho + \frac{1}{12} + \frac{1}{180\lambda_\rho}$. In [CE42, Sect. 4] it was found that $C_2^{\mathrm{FR}}(N,\cdot)$ has zeros off the line. This paper studies those zeros as a function of N, compares ζ with two controls, and asks where the Euler product enters.

1.2. **Results and their status.**

(1) *Hermite–Biehler form and recursion* (Section 2). $C_2^{\mathrm{FR}} = E_N(s) + E_N(1-s)$ with $E_N(s) = N^{s-1}X_{N-1}(s)$, and $E_{N+1} = (\frac{N+1}{N})^{s-1}(E_N + \frac{1}{N})$ (Lemma 1: proved).
(2) *Genealogy* (Section 3). Off-line zeros of C_2^{FR} for ζ are transient with excursion $\approx 1.1/\sqrt{N}$; for the Davenport–Heilbronn function one is permanent (Table 1, Figure 1: numerical; the mechanism, Proposition 2: proved to first order).
(3) *Coefficient families* (Section 4). Positivity or monotonicity of the coefficients does not force the excursions to shrink (Table 2: numerical).
(4) *Translation law* (Section 5). Proposition 3 (proved) holds at every zero, on or off the line.

(5) *The Epstein control* (Section 6). Off-line zeros of the Epstein zeta function of x^2+5y^2, the translation law with complex slope, and permanent off-line zeros of its C_2^{FR} (Tables 3–4: numerical; the zeros are verified to 10^{-10}).
(6) *The Caceres divisor cross-energy* (Section 7). Theorem 6 and its closed, quotient and phase forms, Proposition 8 (proved); comparison with the Epstein coefficients (numerical).
(7) *Exact counting and rigidity* (Section 8). Proposition 9, Theorem 10 and Corollary 11 (proved); checks against direct counts and observed gaps (numerical).
(8) *The zero set is a Fourier quasicrystal* (Section 9). Theorems 12 and 13: closed-form zero measure, spectrum and extinction rule (proved); 114 Bragg peaks checked against 2723 zeros (numerical).
(9) *Exact supremum and interlacing* (Section 10). Theorem 14 and Corollary 15 (proved); the boundary identity for $m = 12$ (exact value, numerically located maximizer); the density $\delta \approx 0.824$ (existence proved by Erdős–Wintner, value numerical).
(10) *Classification* (Section 11). Theorem 16 (sufficiency proved; necessity sketched through Jessen–Tornehave); the threshold sweep (numerical).
(11) *Operator and statistical mechanics* (Section 12). Theorem 17 (proved; verified to 10^{-12}); the primon gas reading and the corner of the free energy (elementary; numerical).
(12) *Sampling* (Section 13). Corollary 18 (from the Levin–Golovin theorem); Riesz bounds and reconstruction (numerical).
(13) *The bridge* (Section 14). The passage from divisors to sizes is the convergence of partial Euler products in the strip (Proposition 19: proved reduction; the equivalence with RH is classical [Co, KKK]).
(14) *The λ-ladder* (Section 15). Proposition 20 (proved) and Table 7 (numerical).
(15) *The harmonic-function criterion of* [Ca17] (Section 16). Proposition 21 (proved) corrects the limit; Table 8 (numerical); Proposition 22 (proved) identifies the off-line oscillation with $\zeta(s)$.
(16) *What C_2^{FR} can decide* (Section 18). Lemma 24 and Proposition 25 (proved) with the zeros of T_N (numerical); the nodal count of C_2 (numerical, with the argument principle); Proposition 26 (proved).
(17) *The prime cross-energy* (Section 17). The identity (8) (classical, by Möbius inversion) and the ladder of singular lines (Proposition 23: proved).

What is classical: Fourier quasicrystals from stable polynomials and the spectra of quantum graphs [KS, ACV, GS]; Clark's perturbations [Cl]; the zeros of almost periodic functions [JT]; the Erdős–Wintner theorem [EW]; Lee–Yang zeros and the primon gas [LY, Ju]; sine-type functions and Kadec's theorem [Lev, Kad]; the Eneström–Kakeya theorem [Ka, PS] and Pólya's theorem on cosine polynomials with positive increasing coefficients [Po], which is Theorem 6 for a single prime; the Hermite–Biehler theorem [Le]; the Davenport–Heilbronn examples, including the Epstein zeta function of x^2+5y^2 [DH]; the representation of the prime zeta function by $\log\zeta(ks)$ and its singularities [LW]; the equivalence between convergence of partial Euler products in $\operatorname{Re} s > \frac{1}{2}$ and the generalized Riemann hypothesis for $L(s,\chi)$, $\chi \neq 1$ [Co, KKK]; the hybrid Euler–Hadamard product [GHK]; the sums $\sum_\rho \lambda_\rho^{-k}$ [Vo]. What is new: the recursion and the genealogy of the zeros of C_2^{FR} with the $1/\sqrt{N}$ law and the comparison with two controls; the use of the Epstein function of x^2+5y^2, with its complex off-line zeros, as a control for the translation law and for C_2^{FR} (the Epstein control itself is in [CE41, Sect. 2], with m^2+100n^2 and a real zero, for C_2 and its trichotomy); the divisor cross-energy and Theorem 6; the reduction of Section 14; the ladder as a bracket of each zero by the previous ones; the correction of [Ca17]; the reading of $\log(P(s)P(1-s))$ as a cross-energy over the primes and the band formula (9).

1.3. **Related work by the author.** This paper is Part 43 of the series *Cross-Energy of Dirichlet Partial Sums* [CE0]. The reflected cross-energy and its closed form are in [CE32], the Hurwitz

route in [CE21], the controls (Davenport–Heilbronn, Beurling systems, function fields) in [CE46], the Epstein control for C_2 in [CE41], and the search for square roots of Weil's form, where the off-line zeros of C_2^{FR} first appeared, in [CE42]. The series is surveyed in [CE0]. Each of these is a self-contained preprint; the present paper can be read without them.

2. The Hermite–Biehler form of C_2^{FR}

Put $s = \frac12 + z$. Since $N^{s-1}k^{-s} = (Nk)^{-1/2}(N/k)^z$ and $N^{-s}k^{s-1} = (Nk)^{-1/2}(N/k)^{-z}$,

$$C_2^{\mathrm{FR}}(N, \tfrac12 + z) = \frac{2}{\sqrt{N}} \sum_{k<N} k^{-1/2} \cosh\Big(z \log \frac{N}{k}\Big). \tag{3}$$

It is an even entire function of z, real on the imaginary axis, with positive coefficients $k^{-1/2}$ that increase with the frequency $\log(N/k)$. For $N = 2$ it is $\sqrt{2}\cosh(z\log 2)$, whose zeros $z = i\pi(m+\frac12)/\log 2$ all lie on the critical line.

Write $E_N(s) = N^{s-1}X_{N-1}(s)$. Then $C_2^{\mathrm{FR}}(N,s) = E_N(s) + E_N(1-s)$, the shape of a Hermite–Biehler pair: if $|E_N(s)| > |E_N(1-s)|$ for $\sigma > \frac12$, all zeros of $C_2^{\mathrm{FR}}(N,\cdot)$ lie on $\sigma = \frac12$ [Le, Ch. VII].

Lemma 1 (Recursion)**.** *$E_1 = 0$ and, for $N \ge 1$,*

$$E_{N+1}(s) = \Big(\frac{N+1}{N}\Big)^{s-1}\Big(E_N(s) + \frac{1}{N}\Big).$$

At a zero ρ of ζ, $E_N(\rho) \to \frac{1}{1-\rho}$, which is the asymptotic fixed point of the recursion for every s; in general $E_N(s) - \big(\frac{1}{1-s} - \frac{1}{2N} - \frac{s}{12N^2} + \cdots\big) = \zeta(s)N^{s-1}$, so $\zeta(s)$ is the amplitude of the homogeneous mode N^{s-1}.

Proof. $E_N(s) + \frac1N = N^{s-1}\big(X_{N-1}(s) + N^{-s}\big) = N^{s-1}X_N(s)$, and multiplying by $(\frac{N+1}{N})^{s-1}$ gives $(N+1)^{s-1}X_N(s) = E_{N+1}(s)$. The second statement is the Euler–Maclaurin expansion $X_{N-1}(s) = \zeta(s) + \frac{N^{1-s}}{1-s} - \frac12 N^{-s} - \frac{s}{12}N^{-s-1} + \cdots$ multiplied by N^{s-1} [CE32]. The fixed point: with $r = 1 + \frac1N$, $r^{s-1} = 1 + \frac{s-1}{N} + O(N^{-2})$, so $E = r^{s-1}(E + \frac1N)$ gives $(s-1)E + 1 = 0$ to first order. □

The Hermite–Biehler inequality for E_N fails: C_2^{FR} has zeros off the line [CE42, Sect. 4]. The rest of this paper measures how, and why.

3. Genealogy of the zeros

For each N we locate the zeros of (3) with $0.004 \le \operatorname{Re} z \le 0.45$ and $5 < \operatorname{Im} z < 100$ (grid minima of $|C_2^{\mathrm{FR}}|$ refined by Newton's method to $|C_2^{\mathrm{FR}}| < 10^{-9}$). By symmetry it suffices to take $\operatorname{Re} z > 0$. The same construction applies to any real coefficient sequence a_k, replacing $k^{-1/2}$ by $a_k k^{-1/2}$; for the Davenport–Heilbronn function f the coefficients are periodic modulo 5, $(a_0,\dots,a_4) = (0, 1, \kappa_0, -\kappa_0, -1)$ [CE13, Sect. 9].

Table 1. Off-line zeros of $C_2^{\mathrm{FR}}(N,\cdot)$, $5 < t < 100$. Maximum of σ in each range of N; for f the permanent zero is listed separately.

range of N	ζ: max σ	f: max σ (transient)	f: permanent zero
2–30	0.914	0.940	intermittent
30–60	0.662	0.919	intermittent
60–100	0.608	0.726	0.80–$0.85 + 85.70i$ from $N = 74$
100–160	0.592	0.625	0.79–$0.84 + 85.70i$

For ζ the off-line zeros appear and disappear from one N to the next, always near the ordinates of zeros of ζ (14.1, 21.0, 25.0, 30.4, 32.9, 37.6, 40.9, 43.3, 48.0, 49.8, …). Restricting to $5 < t < 60$:

$$\max(\sigma - \tfrac{1}{2}) = 0.144 \ (N \approx 40), \quad 0.089 \ (N \approx 120), \quad 0.063 \ (N = 300),$$

0.050 at $N \approx 360$ and 0.033 at $N = 1200$, and $\sqrt{N}\max(\sigma - \frac{1}{2}) = 1.03, 1.09, 1.14$ at $N = 130, 300, 1200$: the excursion decays like $1.1/\sqrt{N}$ (Figure 1). The number of off-line zeros in $5 < t < 60$ stays near one per value of N.

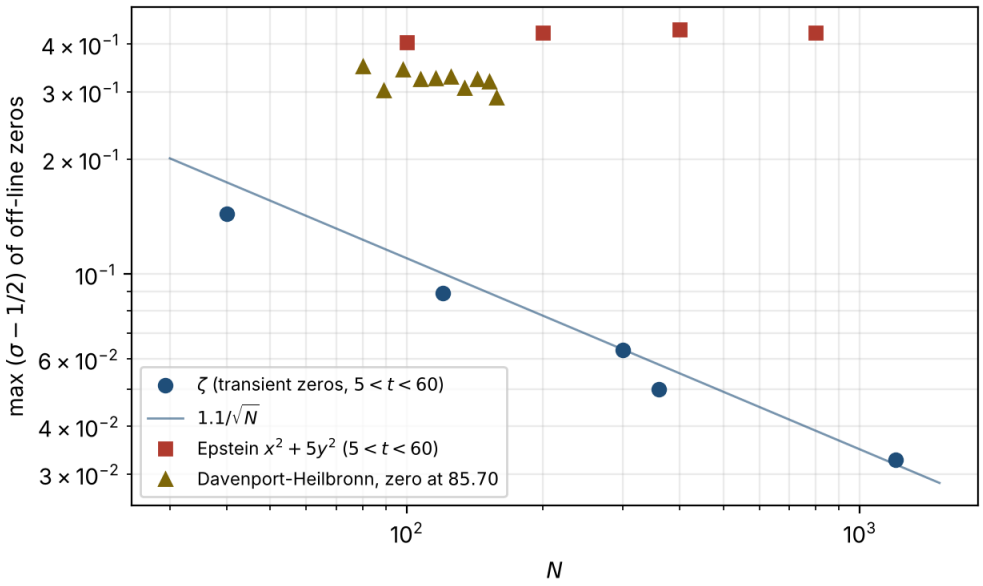

FIGURE 1. Largest distance to the line of the off-line zeros of $C_2^{\mathrm{FR}}(N, \cdot)$. For ζ the zeros are transient and approach the line like $1.1/\sqrt{N}$; for the Davenport–Heilbronn function and for the Epstein zeta function of $x^2 + 5y^2$ they do not.

Proposition 2 (Mechanism). *Let* $A_N(z) = \zeta(\frac{1}{2} + z)N^z + \zeta(\frac{1}{2} - z)N^{-z}$. *Then*

$$C_2^{\mathrm{FR}}(N, \tfrac{1}{2} + z) = \Big(\frac{1}{\lambda} - \frac{1}{N} + \cdots\Big) + N^{-1/2}A_N(z), \qquad A_N(z) = \Xi(z)\Big(\frac{N^z}{G(\frac{1}{2} + z)} + \frac{N^{-z}}{G(\frac{1}{2} - z)}\Big),$$

with $G(s) = \frac{1}{2}s(s-1)\pi^{-s/2}\Gamma(\frac{s}{2})$ *and* $\Xi(z) = \xi(\frac{1}{2} + z)$. *The second factor has all its zeros on the line for* $|t| < 2\pi N^2$ *approximately (Hermite–Biehler for* $E(z) = N^z/G(\frac{1}{2} + z)$*). Hence the zeros of the arithmetic part are those of* ξ *together with a family of points on the line which move with* N. *At a simple zero* ρ *on the line, the first-order displacement of the nearby zero of* C_2^{FR} *is* $\delta = -(\frac{1}{\lambda} - \frac{1}{N})/\partial_s C_2^{\mathrm{FR}}(N, \rho)$, *which is purely imaginary, so the zero stays on the line; it leaves the line only near a collision with a moving zero, where* $\partial_s C_2^{\mathrm{FR}}$ *is small, and the size of the perturbation relative to* A_N *is* $N^{1/2} \cdot N^{-1} = N^{-1/2}$.

Proof. The decomposition is (2) with $\zeta(s) = \xi(s)/G(s)$ and $\xi(\frac{1}{2} + z) = \xi(\frac{1}{2} - z)$. For $E(z) = N^z/G(\frac{1}{2} + z)$, $|E(z)/E(-z)| = N^{2x}|G(\frac{1}{2} - z)/G(\frac{1}{2} + z)| \approx (2\pi N^2/t)^x$ by Stirling, which exceeds 1 for $x > 0$ when $t < 2\pi N^2$. On the line $\frac{1}{\lambda} - \frac{1}{N}$ is real. Up to the Bernoulli terms, $\partial_s C_2^{\mathrm{FR}}(N, \rho) = N^{-1/2}\big(\zeta'(\rho)N^{i\gamma} - \zeta'(1-\rho)N^{-i\gamma}\big) + \frac{2s-1}{\lambda_s^2}\big|_{s=\rho}$. Since $\zeta'(1-\rho) = \zeta'(\bar{\rho}) = \overline{\zeta'(\rho)}$, the first term is $2iN^{-1/2}\,\mathrm{Im}\,\big(\zeta'(\rho)N^{i\gamma}\big)$, and the second is $2i\gamma/\lambda^2$. Both are purely imaginary, so δ is purely imaginary. □

The picture is a stream of zeros moving down the line as N grows (the zeros of the Gamma factor) and fixed rocks (the zeros of ξ). At each passage the term $-\frac{1}{N}$, the shadow of the pole, can push a pair off the line by $O(N^{-1/2})$. A rock off the line, as for f, is not moved by any passage.

4. Coefficient families

To see whether the shrinking is a property of the coefficients, we keep the frequencies $\log(N/k)$ and change a_k.

Table 2. $\max(\sigma - \frac{1}{2})$ over off-line zeros of the cosine sum with coefficients $a_k k^{-1/2}$, $5 < t < 60$, six consecutive values of N.

coefficients a_k	$N \approx 40$	$N \approx 120$	$N \approx 360$
1 (ζ)	0.144	0.089	0.050
Davenport–Heilbronn (no off-line zero below $t = 60$)	0.277	0.092	0.075
positive, random in $[1, 1.6]$	0.302	0.218	0.259
k (decreasing with the frequency)	0.419	0.085	0.434

Positive coefficients that increase with the frequency up to noise do not shrink. The excursions shrink when, and only when, the limit function has its zeros on the line in the window. The Pólya–Kakeya direction of (3) (coefficients increasing with the frequency) is not the mechanism; the density of frequencies, $\propto e^{-u/2}$ in $u = \log(N/k)$, decreases, and no positive average over N changes this, since each $C_2^{\mathrm{FR}}(N, \cdot)$ contributes a decreasing density.

5. The translation law

Proposition 3 (All zeros are one)**.** *Let ρ be any zero of ζ in the strip and $\lambda = \rho(1-\rho)$. Then*

$$X_n(\rho)X_n(1-\rho) = \frac{n}{\lambda} + \frac{1}{2\lambda} + \frac{1}{12n} + O_\rho(n^{-2}),$$

equivalently $\lambda X_n(\rho)X_n(1-\rho) = n + \frac{1}{2} + \frac{\lambda}{12n} + \cdots$. On the line $X_n(1-\rho) = \overline{X_n(\rho)}$, the left side is $|X_n(\rho)|^2$, $\lambda = \frac{1}{4} + \gamma^2$ is real, and in the variable $u = n/\lambda$ every zero follows the same profile $u + \frac{1}{2\lambda} + \cdots$; at C_2^{FR} level the crossing is $N^* = \lambda + \frac{1}{12} + \frac{1}{180\lambda}$.

Proof. With $X_n(s) = \zeta(s) + \frac{n^{1-s}}{1-s} + \frac{1}{2}n^{-s} - \frac{s}{12}n^{-s-1} + \cdots$ and $\zeta(\rho) = \zeta(1-\rho) = 0$, multiply the expansions at ρ and $1-\rho$: the leading term is $\frac{n}{\rho(1-\rho)}$; the constant term is $\frac{1}{2}\big(\frac{1}{1-\rho} + \frac{1}{\rho}\big) = \frac{1}{2\lambda}$; the n^{-1} terms are $\frac{1}{4} - \frac{1}{12} - \frac{1}{12} = \frac{1}{12}$. □

The proof uses only $\zeta(\rho) = \zeta(1-\rho) = 0$. The line enters only through $X_n(1-\rho) = \overline{X_n(\rho)}$. For a zero off the line the law holds with complex λ, and the rescaling $n \mapsto n\lambda'/\lambda$ between two zeros is real exactly when both λ are real. A law of this kind cannot by itself exclude zeros off the line; Section 6 shows a function that realizes it off the line.

6. The Epstein control

Let $E(s) = \zeta(s)L(s, \chi_{-20}) + L(s, \chi_{-4})L(s, \chi_5)$, a multiple of the Epstein zeta function of $x^2 + 5y^2$. It has a simple pole at $s = 1$ with residue $c = L(1, \chi_{-20}) = 2\pi/\sqrt{20}$, the functional equation of a degree-two function of conductor 20, nonnegative coefficients $a(n) = \sum_{d|n} \big(\chi_{-20}(d) + \chi_{-4}(d)\chi_5(n/d)\big)$ $(2, 0, 0, 2, 2, 4, 0, 0, 6, \dots)$, and no Euler product; it is the classical example of Davenport and Heilbronn [DH]. The paper [CE41, Sect. 2] already used an Epstein function, that of $m^2 + 100n^2$ with a real zero, as a control for C_2; here we need complex zeros off the line, to test the translation law and the zeros of C_2^{FR} at a given height.

TABLE 3. Zeros of $E(s)$ off the line with $5 < t < 100$ found by grid search and `findroot`, $|E| < 10^{-10}$.

$0.93767 + 29.98340i$	$0.82319 + 44.00011i$	$0.63491 + 46.75841i$	$0.59744 + 52.74327i$
$0.79978 + 61.14026i$	$0.72485 + 64.99194i$	$0.84547 + 75.34001i$	$0.80772 + 79.41954i$
$0.90799 + 89.55983i$	$0.85028 + 96.10717i$		

With $X_n^E(s) = \sum_{k \le n} a(k) k^{-s}$ and $Q_n = X_n^E(\rho) X_n^E(1-\rho)$, the analogue of Proposition 3 holds with c^2:

TABLE 4. The translation law at two off-line zeros of E: $\lambda Q_n/(c^2 n) \to 1$ and $\arg Q_n \to -\arg \lambda$.

zero	n	$\lambda Q_n/(c^2 n)$	$\arg Q_n$	$-\arg \lambda$
$0.938 + 29.98i$	10^4	$1.0063 - 0.0002i$	0.0290	0.0292
	10^5	$1.0004 - 0.0000i$	0.0292	0.0292
	$2 \cdot 10^5$	$0.9996 + 0.0000i$	0.0292	0.0292
$0.635 + 46.76i$	10^4	$1.0180 - 0.0001i$	0.0056	0.0058
	$2 \cdot 10^5$	$0.9993 + 0.0000i$	0.0058	0.0058

The C_2^{FR} built from $a(n)$ keeps off-line zeros that do not shrink: $\max(\sigma - \frac{1}{2})$ is 0.404, 0.429, 0.436, 0.428 at $N = 100, 200, 400, 800$ for $5 < t < 60$, with zeros at 0.84–$0.92 + 44.0i$ and 0.79–$0.90 + 58.5i$ present at every N tested (Figure 1).

Corollary 4. *A pole at $s = 1$, the functional equation $s \leftrightarrow 1 - s$, nonnegative coefficients and the translation law of Proposition 3 are compatible with zeros off the line. Any argument built from C_2^{FR} that does not use the Euler product cannot prove the Riemann hypothesis.*

7. The Caceres divisor cross-energy

Variables and parameters. Table 5 fixes the notation of this section; every symbol is defined there before it is used.

The sum X_{N-1} cuts the Dirichlet series by size, $n < N$. With an Euler product one may cut by divisors.

Definition 5. Let $m = \prod_p p^{K_p - 1}$ ($K_p \ge 1$, finitely many $K_p > 1$) and $M = \prod_{K_p \ge 2} p^{K_p} = m \operatorname{rad}(m)$. Put

$$E_m(s) = M^{s-1} \sum_{d \mid m} d^{-s} = \prod_{p \mid m} E_p(s), \qquad E_p(s) = p^{K_p(s-1)} \sum_{k < K_p} p^{-ks},$$

and $D_m(s) = E_m(s) + E_m(1-s)$, the *Caceres divisor cross-energy*. The factorization is the Euler product of ζ restricted to the divisors of m; E_p is the cross-energy of a single prime, C_2^{FR} with $N = p^{K_p}$ and the sum restricted to powers of p.

Theorem 6. *For every m, all the zeros of D_m lie on $\operatorname{Re} s = \frac{1}{2}$.*

Proof. Fix p and $K = K_p$, and put $\zeta_p = p^{s - 1/2}$, so that $|\zeta_p| = p^{\sigma - 1/2}$. Then

$$E_p(s) = p^{-K} \sum_{j=1}^{K} p^{j/2} \zeta_p^{\,j} = p^{-K} R(\zeta_p), \qquad E_p(1-s) = p^{-K} R(1/\zeta_p), \qquad R(w) = \sum_{j=1}^{K} p^{j/2} w^j,$$

TABLE 5. Variables and parameters of the Caceres divisor cross-energy.

Symbol	Meaning
$s = \sigma + it$	complex variable; $\sigma = \operatorname{Re} s$ is the horizontal coordinate, $t = \operatorname{Im} s$ the height.
$z = s - \frac{1}{2}$	variable centred on the critical line; $\operatorname{Re} z = 0$ is the line $\operatorname{Re} s = \frac{1}{2}$.
$m \geq 1$	the integer whose divisors are used; it is the only parameter of D_m.
$p \mid m$	a prime dividing m; all products $\prod_{p\mid m}$ run over these primes.
a_p	the exponent of p in m: $m = \prod_{p\mid m} p^{a_p}$, $a_p \geq 1$.
$K_p = a_p + 1$	the number of divisors of m that are powers of p $(1, p, \dots, p^{a_p})$.
$\operatorname{rad}(m) = \prod_{p\mid m} p$	the radical of m, the product of its distinct primes.
$M = m \operatorname{rad}(m)$	the scale, $M = \prod_{p\mid m} p^{K_p}$; it plays the role of N in $C_2^{\mathrm{FR}}(N, s)$ and fixes the density $\log M/\pi$ of zeros per unit of height.
$d \mid m$	a divisor of m; the Dirichlet sum is cut to these d instead of to $n < N$.
$a(d)$	the coefficients on the divisors: $a(d) = 1$ (Euler product of ζ); $a(d) = r_Q(d)$ only in the control.
$r_Q(n)$	control coefficients: the number of $(x, y) \in \mathbb{Z}^2$ with $x^2 + 5y^2 = n$ (Epstein zeta function, no Euler product).
$\sigma_{-s}(m)$	the divisor function at $-s$, $\sigma_{-s}(m) = \sum_{d\mid m} d^{-s}$ (not to be confused with $\sigma = \operatorname{Re} s$), so $\sigma_{s-1}(m) = \sum_{d\mid m} d^{s-1}$.
$E_m(s)$	the first half of D_m: $E_m(s) = M^{s-1}\sigma_{-s}(m)$ (the second half is $E_m(1-s)$).
$E_p(s)$	the factor of E_m at the prime p: $E_p(s) = p^{K_p(s-1)} \sum_{k<K_p} p^{-ks}$, the cross-energy of a single prime.
$A_p(s)$	the closed form of E_p: $A_p(s) = p^{\,s-K_p}(p^{K_p s} - 1)/(p^s - 1)$, so $E_m = \prod_{p\mid m} A_p$.
$D_m(s)$	the Caceres divisor cross-energy, $D_m(s) = E_m(s) + E_m(1-s)$; it satisfies $D_m(s) = D_m(1-s)$.
$\zeta_p = p^{s-1/2}$	the variable of the prime p in the proof of Theorem 6; $\lvert\zeta_p\rvert = p^{\sigma-1/2}$, equal to 1 exactly on the line.
$R(w)$	the polynomial of the prime p, $R(w) = \sum_{j=1}^{K} p^{j/2} w^j$ $(K = K_p)$ with $E_p(s) = p^{-K} R(\zeta_p)$; its coefficients increase by the ratio $\sqrt{p}$, and Eneström–Kakeya puts its zeros in $\lvert w\rvert \leq 1$.
$R^*(w)$	the reciprocal polynomial of R, $R^*(w) = w^K \overline{R(1/\bar{w})}$.
$b_p(s)$	the Blaschke-type factor of p, $b_p(s) = A_p(1-s)/A_p(s)$: $\lvert b_p\rvert < 1$ for $\sigma > \frac{1}{2}$, $\lvert b_p\rvert = 1$ for $\sigma = \frac{1}{2}$.
$B_m = \prod_{p\mid m} b_p$	the quotient $E_m(1-s)/E_m(s)$; $D_m = E_m(1 + B_m)$, so the zeros are the solutions of $B_m = -1$.
$\theta_p = t \log p$	the angle of the prime p at height t on the line.
$\Phi_m(t)$	the phase of $E_m(\frac{1}{2} + it)$: $\sum_{p\mid m}[\theta_p + \arg(p^{K_p/2} e^{iK_p\theta_p} - 1) - \arg(\sqrt{p}\, e^{i\theta_p} - 1)]$; $D_m(\frac{1}{2} + it) = 2\lvert E_m\rvert \cos \Phi_m$.
$k \in \mathbb{Z}$	the index of the zeros on the line, $\Phi_m(t) = \frac{\pi}{2} + k\pi$.
$u = z \log p$	the scaled variable of a single prime in Proposition 8(iii).
$\rho = \frac{1}{2} + i\gamma_\rho$	a zero on the critical line, $\gamma_\rho > 0$ its ordinate.
$\rho = \beta + i\gamma$	a zero off the line, $\beta \neq \frac{1}{2}$, $\gamma > 0$; its mirror is $1 - \bar{\rho} = 1 - \beta + i\gamma$.

where $j = K - k$. The coefficients of $R(w)/w = \sum_{j=0}^{K-1} p^{(j+1)/2} w^j$ are positive and increasing, so by the Eneström–Kakeya theorem [Ka, PS] all zeros of R lie in $\lvert w\rvert \leq 1$. Let $R^*(w) = w^K \overline{R(1/\bar{w})}$. Since the zeros of R lie in the closed unit disc, R/R^* is a finite Blaschke-type quotient with $\lvert R(w)\rvert \geq \lvert R^*(w)\rvert$ for $\lvert w\rvert \geq 1$, and R has no zeros in $\lvert w\rvert > 1$. As the coefficients of R are real, $\lvert R(1/w)\rvert = \lvert R(1/\bar{w})\rvert = \lvert w\rvert^{-K} \lvert R^*(w)\rvert$. Hence for $\lvert w\rvert > 1$

$$\lvert R(1/w)\rvert = \lvert w\rvert^{-K} \lvert R^*(w)\rvert < \lvert R^*(w)\rvert \leq \lvert R(w)\rvert,$$

with strict inequality also when $R^*(w) = 0$, since then $R(w) \neq 0$. With $w = \zeta_p$ this is $|E_p(s)| > |E_p(1-s)|$ for $\sigma > \frac{1}{2}$. Multiplying over $p \mid m$, $|E_m(s)| > |E_m(1-s)|$ for $\sigma > \frac{1}{2}$, so $D_m(s) \neq 0$ there; by the symmetry $D_m(s) = D_m(1-s)$, also for $\sigma < \frac{1}{2}$. □

Remark 7. For a single prime this is Pólya's theorem [Po]: a cosine polynomial with positive increasing coefficients has only real zeros, proved through Eneström–Kakeya. What Theorem 6 adds is the product over $p \mid m$ and the fact that the Euler product supplies, at every prime, exactly the ratio that Pólya's theorem needs. The line is placed at $\frac{1}{2}$ by the ratio $\sqrt{p}$ between consecutive coefficients of R: Eneström–Kakeya puts the zeros of R in $|w| \leq 1$, and $|w| = p^{\sigma-1/2}$. Primes with $K_p = 1$ may be added as factors p^{s-1}, for which $|p^{s-1}| > |p^{-s}|$ when $\sigma > \frac{1}{2}$.

Proposition 8 (closed form)**.** *Let $m = \prod_{p|m} p^{a_p}$, $K_p = a_p + 1$ and $M = \prod_{p|m} p^{K_p}$. Then $E_m(s) = \prod_{p|m} A_p(s)$ with*

$$A_p(s) = p^{K_p(s-1)}\,\frac{1-p^{-K_p s}}{1-p^{-s}} = p^{\,s-K_p}\,\frac{p^{K_p s}-1}{p^s-1},$$

so that

$$D_m(s) = \prod_{p|m} p^{\,s-K_p}\frac{p^{K_p s}-1}{p^s-1} + \prod_{p|m} p^{\,1-s-K_p}\frac{p^{K_p(1-s)}-1}{p^{1-s}-1}.$$

(i) Quotient form. $D_m(s) = E_m(s)\,\big[1 + B_m(s)\big]$ *with*

$$B_m(s) = \prod_{p|m} b_p(s), \qquad b_p(s) = \frac{A_p(1-s)}{A_p(s)} = p^{\,1-2s}\,\frac{(p^{K_p(1-s)}-1)(p^s-1)}{(p^{K_p s}-1)(p^{1-s}-1)}.$$

The zeros of D_m are the solutions of $B_m(s) = -1$. Each b_p satisfies $|b_p(s)| < 1$ for $\sigma > \frac{1}{2}$ and $|b_p(s)| = 1$ for $\sigma = \frac{1}{2}$, so B_m is a finite product of Blaschke-type factors, one for each prime, and Theorem 6 reads: for $\sigma > \frac{1}{2}$, $|B_m(s)| < 1$, hence $B_m(s) \neq -1$.

(ii) Phase on the critical line. *With $\theta_p = t \log p$,*

$$D_m(\tfrac{1}{2}+it) = 2\,\big|E_m(\tfrac{1}{2}+it)\big|\cos\Phi_m(t), \qquad \Phi_m(t) = \sum_{p|m}\Big[\theta_p + \arg\big(p^{K_p/2}e^{iK_p\theta_p}-1\big) - \arg\big(\sqrt{p}\,e^{i\theta_p}-1\big)\Big],$$

and the zeros of D_m are the solutions of $\Phi_m(t) = \frac{\pi}{2} + k\pi$, $k \in \mathbb{Z}$: the phase is a sum of independent phases, one for each prime.

(iii) One prime. *For $m = p^a$, $K = a + 1$, with $u = z \log p$,*

$$D_{p^a}(\tfrac{1}{2}+z) = 2p^{-K/2}\sum_{k=0}^{K-1} p^{-k/2}\cosh\big((K-k)u\big);$$

for $m = p$ the zeros on the line are the solutions of $\cos 2\theta + p^{-1/2}\cos\theta = 0$, $\theta = t \log p$.

Proof. $\sigma_{-s}(p^a) = \sum_{k=0}^{a} p^{-ks} = (1-p^{-Ks})/(1-p^{-s})$ and multiplicativity give the product, and $A_p(1-s)$ is the same expression at $1-s$. (i) is the quotient of the two products; $|b_p| < 1$ for $\sigma > \frac{1}{2}$ is the inequality $|E_p(1-s)| < |E_p(s)|$ of the proof of Theorem 6, and on the line $A_p(1-s) = \overline{A_p(s)}$ since $1 - s = \bar{s}$ and the coefficients are real. (ii) On the line $E_m(1-s) = \overline{E_m(s)}$, so $D_m = 2\,\mathrm{Re}\,E_m$; writing $p^s = \sqrt{p}\,e^{i\theta_p}$ and $p^{K_p s} = p^{K_p/2}e^{iK_p\theta_p}$ in A_p, the positive factors $p^{1/2-K_p}$ do not change the argument. (iii) is $E_p(s) = p^{K(s-1)}\sum_{k<K} p^{-ks}$ at $s = \frac{1}{2} + z$ added to its reflection; for $K = 2$, $A_p(\frac{1}{2}+it) = p^{-3/2}(\sqrt{p}\,e^{2i\theta} + e^{i\theta})$, whose real part vanishes when $\cos 2\theta + p^{-1/2}\cos\theta = 0$. □

Numerically, the closed form, the quotient form and the phase form agree with the divisor sum to relative error 10^{-13} for $m = 2, 12, 360, 5040$ at points on and off the line; for $m = 2$ the first zeros are $t = 1.4224$, 3.9006, 5.1640, 7.6422; and, for example, $|B_{5040}(0.9 + 1.383i)| = 8 \cdot 10^{-6}$.

For $m = 2^4 \cdot 3^2 \cdot 5 \cdot 7$ together with the factors of 11 and 13 ($M = 151\,351\,200$, 60 divisors), on $0.505 \le \sigma \le 1.5$, $0.5 \le t \le 60$:

coefficients on the divisors	$\min \lvert E(s)\rvert/\lvert E(1-s)\rvert$	off-line zeros found
1 (Euler product of ζ)	1.178	0
$a(d)$ of the Epstein function	0.072	12 (e.g. $0.893 + 1.38i$, $0.546 + 7.17i$)

The Epstein coefficients do not factor over the primes, and the divisor cut loses the inequality. Theorem 6 separates ζ from the Epstein control, which Corollary 4 shows that pole, functional equation and positivity cannot do.

The three pictures. Figures 2–4 show the Caceres divisor cross-energy in the complex plane, on the critical line and through its quotient form. They are produced by the ancillary script `plot_divisor_cross_energy.py`, which evaluates D_m by the divisor sum, locates the zeros by Newton's method from the local minima of $\log \lvert D_m\rvert$ on a grid, and refines the zeros on the line by bisection.

In the complex plane (Figure 2) we take $m = 5040 = 2^4 \cdot 3^2 \cdot 5 \cdot 7$, so $M = m\,\mathrm{rad}(m) = 1\,058\,400$, and the rectangle $-0.6 \le \sigma \le 1.6$, $0 < t < 32$. With the coefficients $a(d) = 1$ every one of the 141 zeros lies on $\mathrm{Re}\, s = \frac{1}{2}$, as Theorem 6 requires; the count agrees with the density $\log M/\pi \approx 4.4$ zeros per unit of height. As a control, the same divisors with the Epstein coefficients $a(d) = r_Q(d)$, which do not factor over the primes, give 14 zeros off the line (right panel); only the factorization of the coefficients differs.

On the critical line (Figure 3) we take $m = 12 = 2^2 \cdot 3$, so $K_2 = 3$, $K_3 = 2$, $M = 72$. By Proposition 8(ii), $D_{12}(\frac{1}{2} + it)$ is real and oscillates inside the band $\pm 2|E_{12}(\frac{1}{2} + it)|$, whose width is the product over $p \mid m$ of the closed-form moduli $|A_p|$. The phase $\Phi_{12}(t)$, taken continuously, increases with t, and each zero is a crossing of a level $\frac{\pi}{2} + k\pi$. There are 16 zeros with $t < 12$, all simple sign changes; the first are

$$t = 0.4697,\ 1.3863,\ 2.1981,\ 2.7733,\ 3.2339,\ 3.8689.$$

The mechanism (Figure 4) is read on the quotient $B_m = E_m(1-s)/E_m(s)$ along a horizontal segment at height $t = 10$. The modulus $|B_m| = \prod_{p|m} |b_p|$ equals 1 only at $\sigma = \frac{1}{2}$ and stays below 1 to the right: each factor is of Blaschke type, and a product of such factors cannot return to modulus 1, so $B_m = -1$ is impossible off the line. The descent steepens as m gains primes and prime powers ($m = 2, 12, 5040$).

Table of zeros. Table 6 lists the first zeros $\rho = \frac{1}{2} + i\gamma_\rho$, $\gamma_\rho > 0$, of D_m for $m = 2$, 12 and 5040. The ordinates are computed by bisection on the real function $D_m(\frac{1}{2} + it)$ in 30-digit arithmetic; the residual $|D_m(\rho)|$ is below 10^{-19} at every listed zero. The ordinates for $m = 2$ repeat with period $2\pi/\log 2 = 9.0647$ (the fifth is the first plus one period), as Proposition 8(iii) predicts, and the zeros for $m = 5040$ have mean spacing close to $\pi/\log M = 0.2265$. The full list (all zeros on the line with $t < 12$ for $m = 2, 12$ and $t < 6$ for $m = 5040$) is in the ancillary file `zeros_divisor_cross_energy.csv`, together with the off-line zeros of the Epstein control.

TABLE 6. First zeros $\rho = \frac{1}{2} + i\gamma_\rho$ of the Caceres divisor cross-energy D_m (coefficients $a(d) = 1$): ordinates γ_ρ.

n	$m = 2$ $(M = 4)$	$m = 12$ $(M = 72)$	$m = 5040$ $(M = 1\,058\,400)$
1	1.42238878	0.46971008	0.14021377
2	3.90060923	1.38630818	0.41874239
3	5.16411105	2.19806602	0.69115686
4	7.64233150	2.77332835	0.95205344
5	10.48710906	3.23388082	1.19471624
6		3.86892878	1.41342599
7		4.69153502	1.60856905
8		5.50869245	1.78814899
9		6.15047258	1.96399931
10		6.85715401	2.14926038

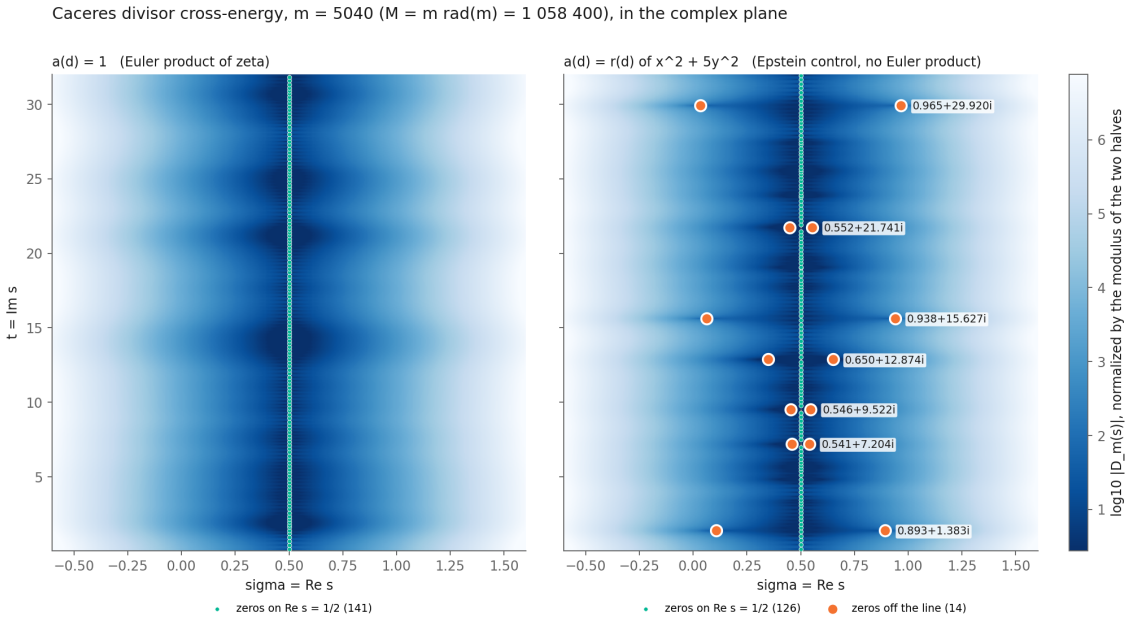

FIGURE 2. $\log_{10}|D_m(s)|$ for $m = 5040$, normalized by the modulus of the two halves, on $-0.6 \le \sigma \le 1.6$, $0 < t < 32$; dark wells are zeros and the dashed line is $\mathrm{Re}\, s = \frac{1}{2}$. Left: $a(d) = 1$, the Euler product of ζ on the divisors; all 141 zeros are on the line (Theorem 6). Right (control): the Epstein coefficients of $x^2 + 5y^2$ on the same divisors; 14 zeros leave the line.

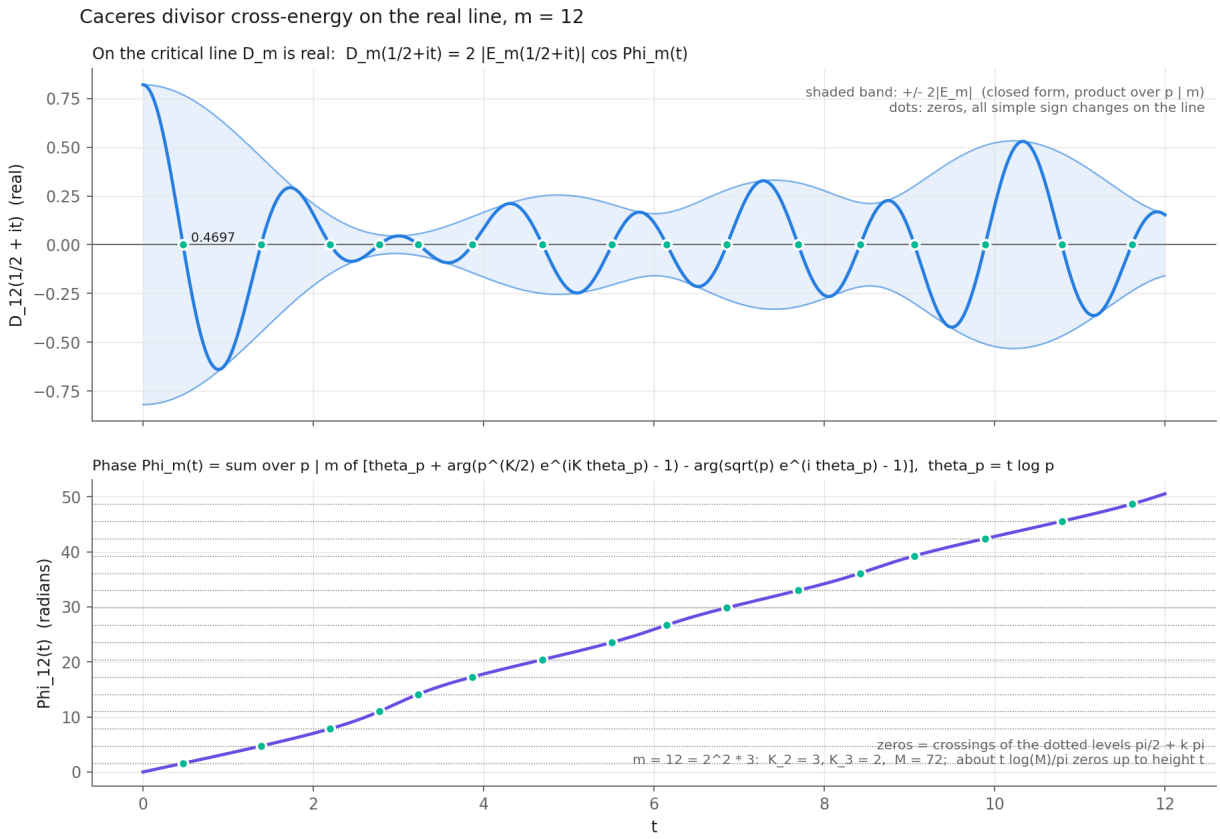

FIGURE 3. The Caceres divisor cross-energy on the critical line, $m = 12$. Top: $D_{12}(\frac{1}{2}+it)$, real, inside the envelope $\pm 2|E_{12}|$ given by the closed form; the dots are its zeros. Bottom: the phase $\Phi_{12}(t)$ of Proposition 8(ii), taken continuously; the zeros are its crossings of the levels $\frac{\pi}{2}+k\pi$ (dotted).

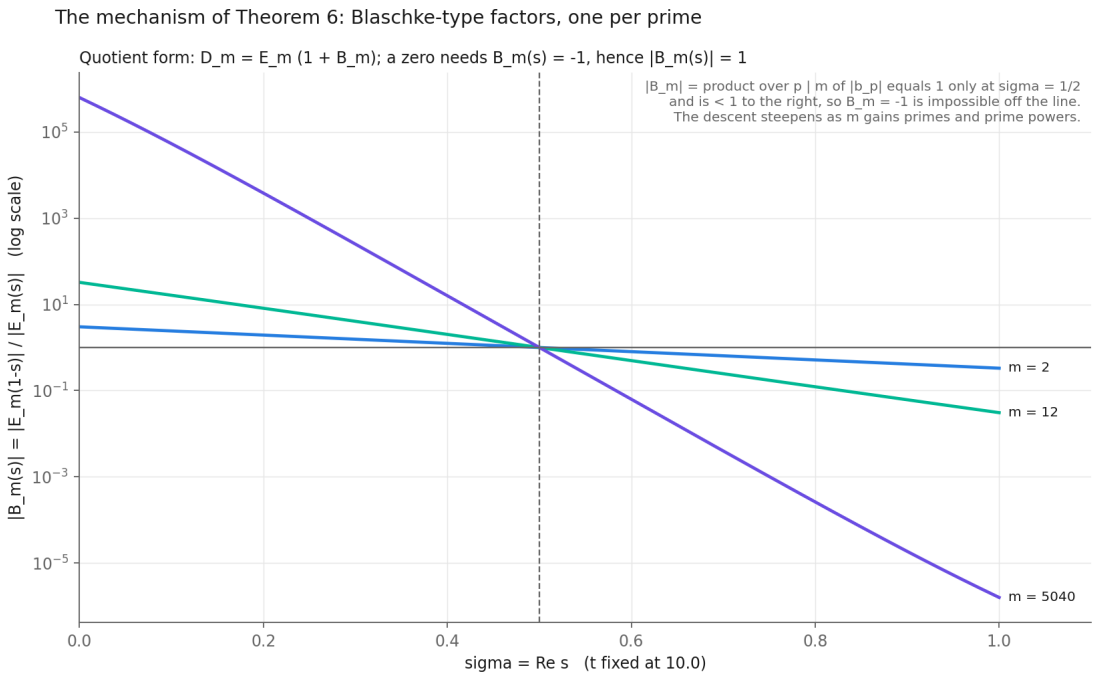

FIGURE 4. The quotient form of Proposition 8(i): $|B_m(\sigma + it)|$ on a logarithmic scale at the fixed height $t = 10$, for $m = 2, 12, 5040$. The modulus crosses 1 only at $\sigma = \frac{1}{2}$ and is < 1 to the right, so $B_m \neq -1$ there.

8. The zeros on the line: exact counting and rigidity

From now on $m \geq 2$ is fixed, $s = \frac{1}{2} + iT$ on the line, and $\theta_p = T \log p$. The local factor of E_m factorizes completely. With $u = p^s$ and $K = K_p$,

$$E_p(s) = p^{K(s-1)} \frac{1 - p^{-Ks}}{1 - p^{-s}} = p^{-K}\, u\, \frac{u^K - 1}{u - 1} = p^{-K}\, u \prod_{\omega^K = 1,\ \omega \neq 1} (u - \omega). \tag{4}$$

So the zeros of E_p are the points $p^s = \omega$, all on $\operatorname{Re} s = 0$, and E_m has no zero in $\operatorname{Re} s > 0$. On the line $u = \sqrt{p}\, e^{i\theta_p}$, and the phase $\Phi_m(T) = \arg E_m(\frac{1}{2} + iT)$ of Proposition 8(ii) becomes a sum of arguments of points moving on circles around fixed centres inside the unit disc:

$$\Phi_m(T) = \sum_{p \mid m} \Big[\theta_p + \sum_{\omega^{K_p} = 1,\ \omega \neq 1} \arg\big(e^{i\theta_p} - \omega p^{-1/2}\big) \Big] + \text{const.} \tag{5}$$

Proposition 9 (the phase is a sum of Poisson kernels)**.** *For every T,*

$$\Phi_m'(T) = \sum_{p \mid m} \log p \, \Big[1 + \sum_{\omega^{K_p} = 1,\ \omega \neq 1} \Big(\frac{1}{2} + \frac{1}{2}\, \frac{1 - p^{-1}}{|e^{i\theta_p} - \omega p^{-1/2}|^2} \Big) \Big] > 0,$$

and, with $r_p = p^{-1/2}$,

$$\sum_{p \mid m} \log p \Big(1 + \frac{K_p - 1}{1 + r_p} \Big) \;\leq\; \Phi_m'(T) \;\leq\; \sum_{p \mid m} \log p \Big(1 + \frac{K_p - 1}{1 - r_p} \Big).$$

The mean value of Φ_m' over T is $\log M$.

Proof. For $|a| < 1$, $\frac{d}{d\theta} \arg(e^{i\theta} - a) = \operatorname{Re} \frac{e^{i\theta}}{e^{i\theta} - a} = \frac{1}{2} + \frac{1}{2}\, \frac{1 - |a|^2}{|e^{i\theta} - a|^2}$, which is positive and lies between $\frac{1}{1+|a|}$ and $\frac{1}{1-|a|}$ because $1 - |a| \leq |e^{i\theta} - a| \leq 1 + |a|$. Apply this to (5) with $|a| = p^{-1/2}$ and multiply by $d\theta_p / dT = \log p$. The Poisson kernel has mean 1 in θ, so the mean of the bracket is K_p, and $\sum_p K_p \log p = \log M$. □

Theorem 10 (exact counting)**.** *Let $N_m(T)$ be the number of zeros $\frac{1}{2} + i\gamma$ of D_m with $0 < \gamma \leq T$, and $S_m(T) = \big(\Phi_m(T) - T \log M\big)/\pi$, with $\Phi_m(0) = 0$. Then*

$$N_m(T) = \Big\lfloor \frac{T \log M}{\pi} + \frac{1}{2} + S_m(T) \Big\rfloor, \qquad S_m(T) = \frac{1}{\pi} \sum_{p \mid m} \Big[\arg\big(1 - p^{-K_p s}\big) - \arg\big(1 - p^{-s}\big) \Big],$$

all zeros are simple, and the n-th zero satisfies $\gamma_n = \frac{\pi}{\log M} \big(n - \frac{1}{2} - S_m(\gamma_n) \big)$.

Proof. On the line $D_m = E_m + \overline{E_m} = 2|E_m| \cos \Phi_m$ and $|E_m| > 0$ there, so the zeros are the solutions of $\Phi_m(T) = \frac{\pi}{2} + k\pi$. By Proposition 9 Φ_m is strictly increasing, so each level is crossed once and transversally. The expression of S_m is $\arg \sigma_{-s}(m)$, since $E_m(\frac{1}{2} + iT) = M^{-1/2} M^{iT} \sigma_{-s}(m)$ and $\sigma_{-s}(p^a) = (1 - p^{-Ks})/(1 - p^{-s})$; each argument is principal because $|p^{-Ks}|, |p^{-s}| < 1$. □

This is a Riemann–von Mangoldt formula with no error term: the smooth term $T \log M / \pi$ plays the role of $\vartheta(T)/\pi$, and S_m is the argument of the Euler product of ζ over the primes of m, each factor cut at p^{a_p}. It was checked against direct sign counts for $m = 12, 5040, 30030, 720720$ ($16, 27, 262, 189$ zeros).

Corollary 11 (rigidity)**.** *The gaps between consecutive zeros, normalized by the mean gap $\pi / \log M$, lie in*

$$\Big[\frac{\log M}{\sum_p \log p \, (1 + \frac{K_p - 1}{1 - r_p})},\ \frac{\log M}{\sum_p \log p \, (1 + \frac{K_p - 1}{1 + r_p})} \Big].$$

The upper end is essentially sharp. For $m = 12$, 5040 and 30030 it gives 1.296, 1.274 and 1.159; the largest normalized gaps among the first 2000 zeros are 1.279, 1.230 and 1.155, and for $m = 30030$ the lower bound of Proposition 9 is attained to three decimals (17.787). The gaps are neither Poisson nor GUE: there are no small gaps and no large ones (Figure 5).

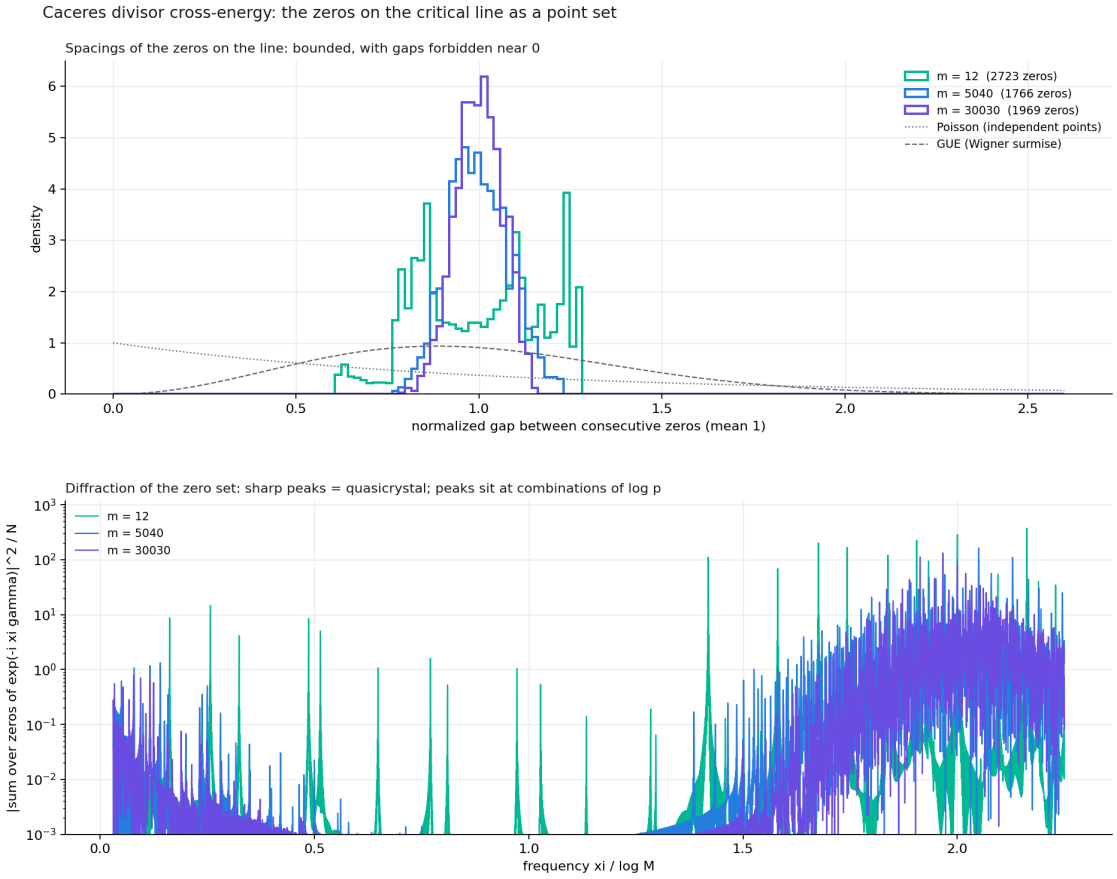

FIGURE 5. Top: normalized gaps between consecutive zeros of D_m on the line, $m = 12, 5040, 30030$ (about 2000 zeros each), against the Poisson and GUE laws: the spacing law is compact. Bottom: the diffraction $|\sum_\gamma e^{-i\xi\gamma}|^2/N$ of the same zero sets, with discrete peaks on a very low background (Section 9).

9. The zero set is a Fourier quasicrystal

Let $z_p = p^{iT} = e^{i\theta_p}$. By (4), on the line $E_m/\overline{E_m}$ is a product of finite Blaschke products, one in each variable z_p:

$$e^{2i\Phi_m(T)} = \frac{E_m(s)}{E_m(1-s)} = \frac{1}{B_m(s)} = \prod_{p|m} \beta_p(z_p), \qquad \beta_p(z) = z^{K_p+1} \prod_{\omega^{K_p}=1,\ \omega\neq 1} \frac{z - \omega p^{-1/2}}{1 - \bar{\omega} p^{-1/2} z}. \tag{6}$$

The zeros of β_p are 0 (with multiplicity $K_p + 1$) and the K_p-th roots of unity other than 1, scaled by $p^{-1/2}$; its degree is $2K_p$.

Theorem 12 (the zero measure in closed form)**.** *Let $\mu_m = \sum_\gamma \delta_\gamma$ be the counting measure of the zeros $\frac{1}{2} + i\gamma$ of D_m, $\gamma \in \mathbb{R}$. Then, as distributions,*

$$N_m(T) = \frac{\Phi_m(T)}{\pi} + \sum_{n\geq 1} \frac{(-1)^n}{\pi n} \operatorname{Im} B_m^{-n}, \qquad \mu_m = \frac{\Phi_m'}{\pi} + \sum_{n\neq 0} \frac{(-1)^n}{2\pi i\, n} \frac{d}{dT} B_m^{-n}.$$

Proof. Since Φ_m is smooth and strictly increasing, $\mu_m = \Phi_m'(T) \sum_k \delta\big(\Phi_m(T) - (k+\frac{1}{2})\pi\big)$, and Poisson summation gives $\sum_k \delta(x - (k+\frac{1}{2})\pi) = \frac{1}{\pi}\sum_n (-1)^n e^{2inx}$. With $e^{2in\Phi_m} = B_m^{-n}$ and $\Phi_m' e^{2in\Phi_m} = \frac{1}{2in}\frac{d}{dT} e^{2in\Phi_m}$ for $n \neq 0$ this is the second formula; the first is its integral, written with $\lfloor x + \frac{1}{2} \rfloor = x + \sum_{n\geq 1} (-1)^n \sin(2\pi n x)/(\pi n)$. □

The variables z_p are independent: since the $\log p$ are linearly independent over $\mathbb{Q}$, the line $T \mapsto (\theta_p)_{p|m}$ is dense in the torus (Kronecker), and every term of Theorem 12 is a function on the torus evaluated along that line. The Fourier transform of μ_m is therefore supported on the frequencies $\lambda_j = \sum_p j_p \log p$, $j \in \mathbb{Z}^{\omega(m)}$, and its coefficients are torus Fourier coefficients.

Theorem 13 (spectrum and extinction rule)**.** *Let $\omega(m) \geq 2$ and write $\mu_m = \sum_j c_j e^{i\lambda_j T}$ (as an almost periodic distribution). Then $c_0 = \log M/\pi$, and $c_j = 0$ unless either*

(1) *j lies on an axis, $j = (0, \dots, 0, j_p, 0, \dots, 0)$, in which case*

$$c_j = \frac{\log p}{2\pi}\, p^{-|j_p|/2} \left(K_p\, \mathbf{1}_{K_p | j_p} - 1\right);$$

(2) *or, for some $n \geq 1$, either $j_p \geq n(K_p+1)$ for every $p \mid m$ or $j_p \leq -n(K_p+1)$ for every $p \mid m$, in which case*

$$c_j = \sum_{n\geq 1:\ j \geq n(K+1)} \frac{(-1)^n \lambda_j}{2\pi n} \Big[\prod_p z_p^{j_p}\Big] \prod_{p|m} \beta_p(z_p)^n$$

for $j > 0$, and $c_{-j} = \overline{c_j}$.

Every other frequency is extinct. In particular the frequency $\log M$ is always extinct.

Proof. The term Φ_m'/π is a sum of functions of one variable each; by Proposition 9 and $\frac{1-r^2}{|e^{i\theta}-a|^2} = \sum_k r^{|k|} e^{ik(\theta-\varphi)}$ ($a = re^{i\varphi}$), its coefficient at $j_p \neq 0$ on the p-axis is $\frac{\log p}{2\pi} r^{|j_p|} \sum_{\omega \neq 1} \bar\omega^{j_p}$, and $\sum_{\omega^K=1, \omega\neq 1} \bar\omega^j = K\mathbf{1}_{K|j} - 1$. Each β_p is analytic in the closed disc with a zero of order $K_p + 1$ at 0, so $B_m^{-n} = \prod_p \beta_p^n$, $n \geq 1$, has Fourier support in $j \geq n(K+1)$; $\frac{d}{dT}$ multiplies the coefficient at j by $i\lambda_j$ and does not move the support; $n \leq -1$ gives the conjugates. When $\omega(m) \geq 2$ the orthants and the axes are disjoint. The point $(K_p)_p$, of frequency $\log M$, is on no axis and has $K_p < K_p + 1$. □

This is a Fourier quasicrystal in the sense of [KS]: μ_m is a positive measure on a uniformly discrete set, and its Fourier transform is a discrete measure. Its spectrum lies on the additive group generated by the $\log p$, $p \mid m$, and the extinction rule says exactly which elements of that group carry no Bragg peak. Theorem 13 was checked for $m = 12$ in two ways (Figure 6): the closed-form coefficients agree with a torus FFT to 6 digits, also at frequencies where the term $n = 2$ contributes, and the predicted intensities $T_0|c_j|^2\pi/\log M$ agree with the diffraction of the 2723 actual zeros below $T_0 = 2000$ at 114 peaks, with median relative error 0.4%.

10. The exact supremum of the counting error and interlacing

Theorem 14 (exact supremum)**.** *For $a \geq 1$ let $H(p,a) = \max_\theta \big|\arg \sum_{k=0}^{a} p^{-k/2} e^{ik\theta}\big|$. Then*

$$\sup_{T\in\mathbb{R}} |S_m(T)| = \frac{1}{\pi} \sum_{p|m} H(p, a_p),$$

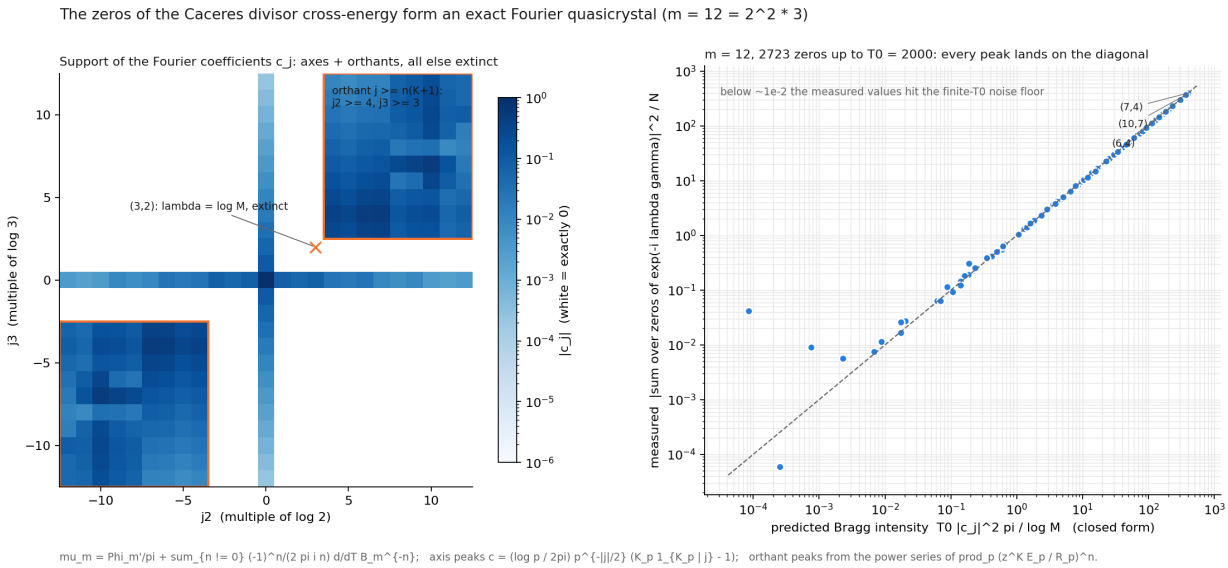

FIGURE 6. $m = 12$. Left: support of the Fourier coefficients c_j, $j = (j_2, j_3)$: the two axes and the orthants $j \geq n(K+1)$ (here $j_2 \geq 4$, $j_3 \geq 3$); white is exactly zero, and the frequency $\log M$ (cross) is extinct. Right: predicted Bragg intensities against the diffraction of 2723 actual zeros.

When $\omega(m) \geq 2$ the supremum is attained only if the maximizing angles θ_p^* of the local terms satisfy $T \log p \equiv \theta_p^* \pmod{2\pi}$ for all $p \mid m$ at a common T, a relation between the θ_p^* and the $\log p$; otherwise it is approached but not attained.

Proof. $\pi S_m(T) = \sum_p h_p(\theta_p)$ with $h_p(\theta) = \arg \sigma_{-1/2-i\theta/\log p}(p^{a_p}) = \arg \sum_{k \leq a_p} p^{-k/2} e^{-ik\theta}$, a continuous odd function of θ. By Kronecker's theorem the values of $(\theta_p \bmod 2\pi)_p$ along $T \in \mathbb{R}$ are dense in the torus, so $\sup_T \sum_p h_p(\theta_p) = \sum_p \max h_p$; the value is reached on the line only at a common T with $T \log p \equiv \theta_p^*$ for all p. □

For $a = 1$, $H(p, 1) = \arcsin p^{-1/2}$, and $H(p, a) \to \arcsin p^{-1/2}$ as $a \to \infty$; in between it is larger (for $p = 2$ the maximum over a is 0.31047π at $a = 3$; for $p \geq 3$ it is at $a = 2$).

Corollary 15 (interlacing)**.** *Each cell $\left[(n-1)\pi/\log M,\ n\pi/\log M\right)$ contains exactly one zero of D_m, equivalently $(-1)^n D_m(\frac{1}{2} + in\pi/\log M) > 0$ for all n, if*

$$\sum_{p \mid m} H(p, a_p) < \frac{\pi}{2},$$

and it fails if the sum exceeds $\frac{\pi}{2}$. In the boundary case the conclusion holds with closed cells, and with open cells unless the supremum of Theorem 14 is attained.

Proof. By Theorem 10, $\gamma_n \log M/\pi = n - \frac{1}{2} - S_m(\gamma_n)$, and at $T = n\pi/\log M$ we have $\cos \Phi_m = (-1)^n \cos(\pi S_m)$. If the sum is $< \frac{\pi}{2}$ then $|S_m| < \frac{1}{2}$ everywhere; if it exceeds $\frac{\pi}{2}$, then $|S_m| > \frac{1}{2}$ on an open set of the torus, which the line visits by Kronecker's theorem. □

The boundary case $m = 12$. Here $H(3, 1) = \arcsin(1/\sqrt{3})$, and $H(2, 2) = \arctan\sqrt{2}$, attained at $\theta = \frac{\pi}{2}$, where $1 + \frac{i}{\sqrt{2}} - \frac{1}{2} = \frac{1}{2} + \frac{i}{\sqrt{2}}$ (the location of the maximum was checked numerically; the value to 30 digits). Since $\arcsin(1/\sqrt{3}) = \arctan(1/\sqrt{2})$,

$$H(2, 2) + H(3, 1) = \arctan\sqrt{2} + \arctan\tfrac{1}{\sqrt{2}} = \frac{\pi}{2}$$

exactly: $m = 12$ is the boundary case. Its zeros come arbitrarily close to the lattice points; the sampled maximum of $|S_{12}|$ over $T \in [1, 10^7]$ is 0.50000, and the lattice signs alternate at all the $2 \cdot 10^5$ lattice points tested. The integers $m < 200$ that do not interlace are $24, 30, 36, 42, 60, 66, 70, 72, 78, 84, 90, \ldots$; 18 and 48 interlace, 24 and 36 do not.

The density of interlacing integers. $f(m) = \sum_{p|m} H(p, a_p)$ is additive and $\sum_p f(p)/p < \infty$, so by the Erdős–Wintner theorem [EW] it has a limiting distribution, and the interlacing integers have a natural density δ. Counting up to x gives 0.8358, 0.8260, 0.8232, 0.8228, 0.8241 for $x = 10^3, \ldots, 10^7$, so $\delta \approx 0.824$ (Figure 7).

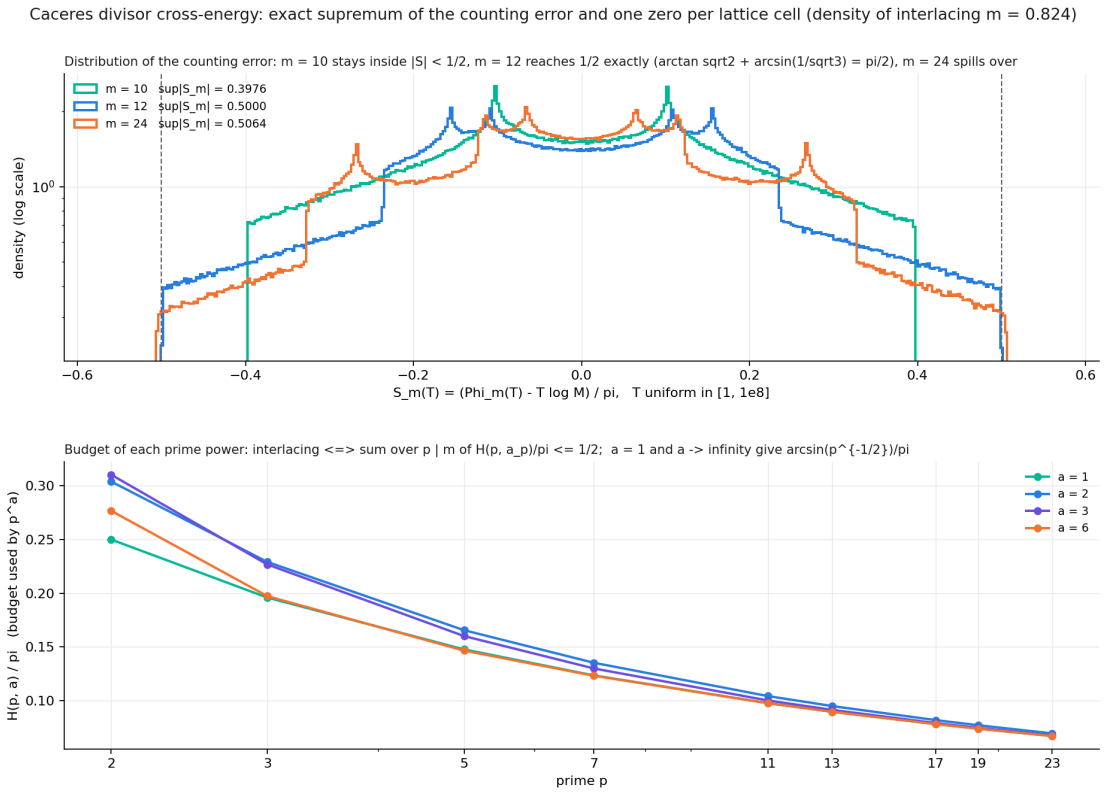

FIGURE 7. Top: distribution of $S_m(T)$ over $T \in [1, 10^8]$ for $m = 10$ (inside $|S| < \frac{1}{2}$), $m = 12$ (reaching $\frac{1}{2}$ exactly) and $m = 24$ (crossing it); the support is compact with sharp edges and singular peaks. Bottom: the budget $H(p, a)/\pi$ of each prime power.

11. Classification: a local Lee–Yang condition

Let a be a real multiplicative function on the divisors of m with $a(1) = 1$, and define

$$E_m^a(s) = M^{s-1} \sum_{d|m} a(d) d^{-s} = \prod_{p|m} E_p^a(s), \qquad E_p^a(s) = p^{K_p(s-1)} \sum_{k<K_p} a(p^k) p^{-ks},$$

$$D_m^a(s) = E_m^a(s) + E_m^a(1-s).$$

The zeros of D_m^a are the solutions of $\prod_p b_p = -1$ with $b_p = E_p^a(1-s)/E_p^a(s)$, and b_p depends on σ and on θ_p only.

Theorem 16 (classification)**.** *Let $\omega(m) \geq 2$. All zeros of D_m^a lie on $\operatorname{Re} s = \frac{1}{2}$ if and only if, for every $p \mid m$, the local polynomial $P_p(x) = \sum_{k \leq a_p} a(p^k) x^k$ has no root in $|x| < p^{-1/2}$; equivalently, no local Euler factor E_p^a vanishes in $\operatorname{Re} s > \frac{1}{2}$.*

Proof. Sufficiency. With $x = p^{-s}$, $E_p^a(s) \neq 0$ in $\sigma > \frac{1}{2}$ means that the roots of P_p lie in $|x| \geq p^{-1/2}$, i.e. that the polynomial $R(w) = \sum_{j=1}^{K} a(p^{K-j}) p^{j/2} w^j$ of the proof of Theorem 6 has its roots in $|w| \leq 1$. The argument of that proof then gives $|E_p^a(s)| > |E_p^a(1-s)|$ for $\sigma > \frac{1}{2}$, so $|\prod_p b_p| < 1$ and $D_m^a \neq 0$ there; by symmetry also for $\sigma < \frac{1}{2}$.

Necessity (sketch). Let $E_p^a(s_0) = 0$ with $\sigma_0 > \frac{1}{2}$. Then b_p has a pole at s_0, so near $(\sigma_0, \theta_p(s_0))$ its modulus takes every large value. Fix σ close to σ_0 and a second prime $q \mid m$. As θ_q runs over the circle, $b_q(\sigma, \theta_q)$ runs over a closed curve that winds around 0, so the phase of $\prod b$ can be adjusted to π while θ_p adjusts the modulus to 1. This gives a zero of the torus function $1 + \prod_p b_p(\sigma, \theta_p)$, isolated and of nonzero index for generic σ, and by the theory of zeros of almost periodic functions (Jessen–Tornehave [JT]) D_m^a has zeros ρ with $\operatorname{Re} \rho$ arbitrarily close to that σ. □

More precisely, the closure of the set of real parts of the zeros of D_m^a in $\sigma > \frac{1}{2}$ is $\{\sigma : \prod_p \min_\theta |b_p| \leq 1 \leq \prod_p \max_\theta |b_p|\}$, with $\max_\theta |b_p| = \infty$ at the real parts of the local zeros. Stable factors cannot compensate an unstable one: adding primes with $a \equiv 1$ only narrows this band. Figure 8 shows the transition for $m = 12$, $a(3) = a(4) = 1$ and $a(2)$ swept through the threshold $a(2) = -3/\sqrt{2}$, where a root of $1 + a(2)x + x^2$ reaches $|x| = 2^{-1/2}$. Above the threshold no zero leaves the line (none found with $t < 150$); below it all the zeros found off the line lie in the predicted band and cluster at the real part $-\log_2 |x_0|$ of the local zero. For a single prime ($\omega(m) = 1$) the criterion is different: $D_{p^a}^a$ is a self-inversive polynomial in $p^{s-1/2}$ and Cohn's theorem applies.

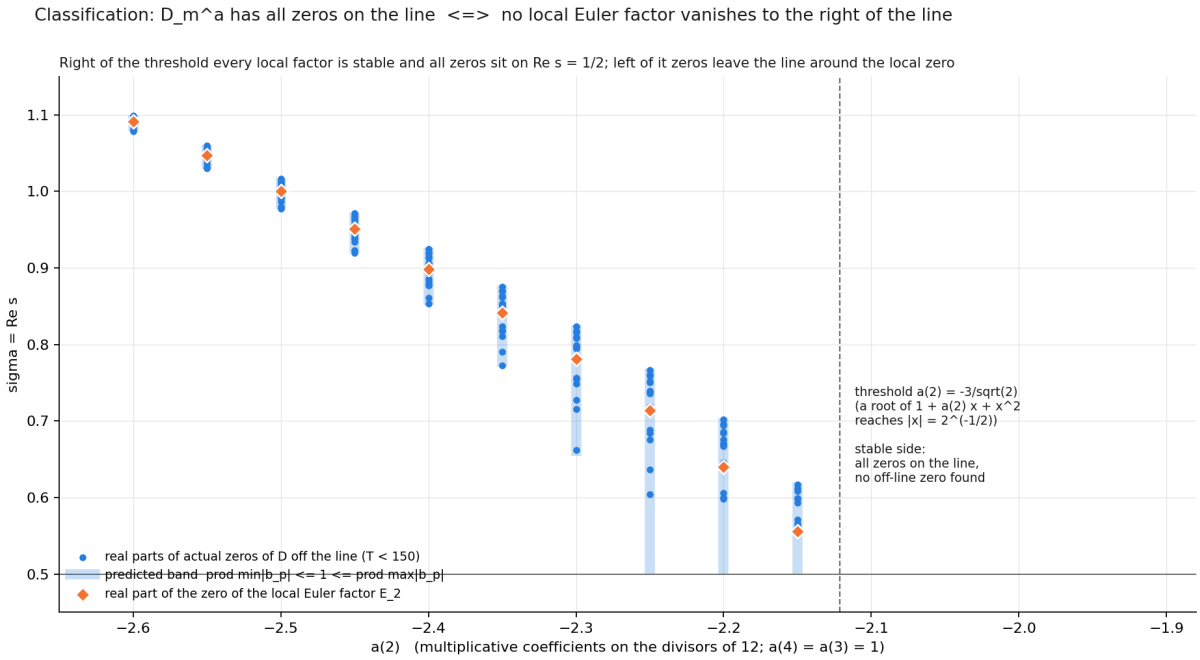

FIGURE 8. Classification for $m = 12$: real parts of the zeros of D_m^a off the line ($t < 150$, dots), predicted band (shaded) and real part of the zero of the local factor E_2^a (diamonds), as $a(2)$ crosses the stability threshold $-3/\sqrt{2}$.

With $a \equiv 1$ every local polynomial is $1 + x + \cdots + x^{a_p}$, whose roots are on $|x| = 1 > p^{-1/2}$: this is Theorem 6 again, and the critical line of the family is the place where every prime, taken alone, is stable. The coefficients of the Epstein zeta function are not multiplicative, so the Epstein construction of Section 7 has no local factors at all.

12. A quantum graph of the primes, and a primon gas

12.1. **The operator.** A finite Blaschke product of degree n is the transfer function of a unitary colligation of size $n+1$. For one factor $(z-\alpha)/(1-\bar\alpha z)$ the colligation is $\begin{pmatrix} \bar\alpha & \sqrt{1-|\alpha|^2} \\ \sqrt{1-|\alpha|^2} & -\alpha \end{pmatrix}$, and the series connection of colligations realizes products. Applied to the $2K_p$ factors of every β_p in (6) this gives a unitary matrix $U = \left(\begin{smallmatrix} A & b \\ c & d \end{smallmatrix}\right)$ of size $N+1$, $N = \sum_p 2K_p$, with

$$d + c\,Z(I - AZ)^{-1}b = B_m^{-1}, \qquad Z(T) = \bigoplus_{p\mid m} p^{iT} I_{2K_p}.$$

Theorem 17 (the zeros are the spectrum of a quantum graph)**.** *Let $U_{-1} = A + b(-1-d)^{-1}c$ (Clark's perturbation [Cl]). Then U_{-1} is unitary and*

$$D_m(\tfrac12 + iT) = 0 \iff \det\big(I - U_{-1}Z(T)\big) = 0.$$

This is the secular equation of a quantum graph with $2K_p$ bonds of length $\log p$ for each $p \mid m$ and vertex scattering matrix U_{-1} [GS]. The total bond length is $2\log M$, and the Weyl law of the graph, $T\log M/\pi$, is the main term of Theorem 10.

Proof. For a unitary colligation, $\tau(Z) = d + cZ(I-AZ)^{-1}b$ equals λ, $|\lambda| = 1$, exactly when $\det(I - (A + b(\lambda - d)^{-1}c)Z) = 0$, and $A + b(\lambda-d)^{-1}c$ is unitary (Clark). Take $\lambda = -1$ and use $B_m^{-1} = -1 \iff D_m = 0$. □

Numerically: U is unitary to 10^{-16}, its transfer function reproduces B_m^{-1} to 10^{-15}, and $|\det(I - U_{-1}Z)| \le 10^{-12}$ at the zeros with $t < 30$ for $m = 12$, 30, 5040 (40, 65, 132 zeros), against values near 2 half a cell away. The eigenphases of $U_{-1}Z(T)$ increase with T (positive bond lengths), and each zero of D_m is a crossing of 0 by one of them (Figure 9). For $m = 12$ the matrix U_{-1} is essentially a ring through all the bonds, with small mixing blocks coming from the zeros $\omega p^{-1/2}$ of β_p. The graph trace formula is a sum over periodic orbits, whose lengths are the λ_j; Theorem 13 lists the orbit lengths that carry weight.

12.2. **A primon gas.** On the space spanned by $|d\rangle$, $d \mid m$, with $H|d\rangle = \log d\,|d\rangle$,

$$Z_m(\beta) = \operatorname{Tr} e^{-\beta H} = \sigma_{-\beta}(m) = \prod_{p\mid m} \frac{1 - p^{-K_p\beta}}{1 - p^{-\beta}}$$

is the partition function of independent modes, one for each prime, with energy $\log p$ per quantum and at most a_p quanta: a finite primon gas [Ju] of parafermions (fermions when m is squarefree). Thus

$$D_m(\beta) = M^{\beta-1}Z_m(\beta) + M^{-\beta}Z_m(1-\beta)$$

is the partition function symmetrized by the duality $\beta \leftrightarrow 1-\beta$. The Fisher zeros of Z_m lie on $\operatorname{Re}\beta = 0$; after symmetrization they all lie on the self-dual line $\operatorname{Re}\beta = \frac12$, and Theorem 6 is a Lee–Yang theorem [LY] for this gas. Theorem 16 is a Lee–Yang condition on each single-mode partition function $P_p(x)$ in the fugacity $x = p^{-\beta}$: no zero in the disc $|x| < p^{-1/2}$.

Along the primorials the free energy per unit of scale has a corner at the self-dual point:

$$\frac{\log D_m(\sigma)}{\log M} \longrightarrow \max(\sigma - 1, -\sigma) \qquad (0 < \sigma < 1),$$

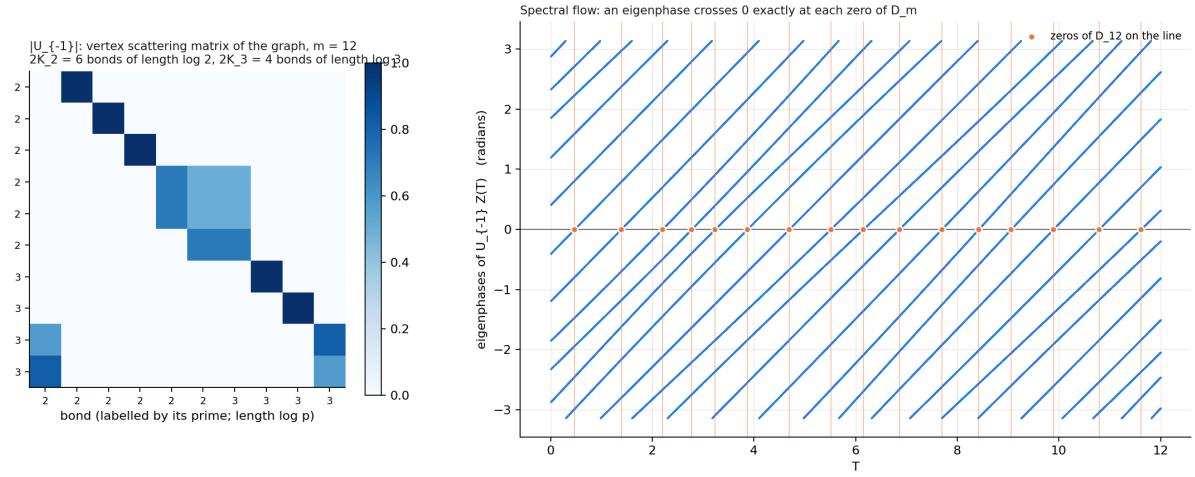

FIGURE 9. $m = 12$. Left: $|U_{-1}|$, the vertex scattering matrix (6 bonds of length $\log 2$, 4 of length $\log 3$). Right: eigenphases of $U_{-1}Z(T)$; each zero of D_{12} (dots) is a crossing of 0.

because $\log Z_m(\sigma) = \sum_{p \le P} \log(1 + p^{-\sigma}) = o(\log M)$. The derivative jumps by 2, which is 2π times the normalized zero density $1/\pi$: Lee–Yang electrostatics for the zeros of Theorem 10. Numerically $f(\frac{1}{2}) = -0.278, -0.467, -0.4985, -0.4999$ and the jump is $0.72, 1.88, 1.987, 1.999$ for the primes up to $10, 10^2, 10^4, 10^6$ (Figure 10).

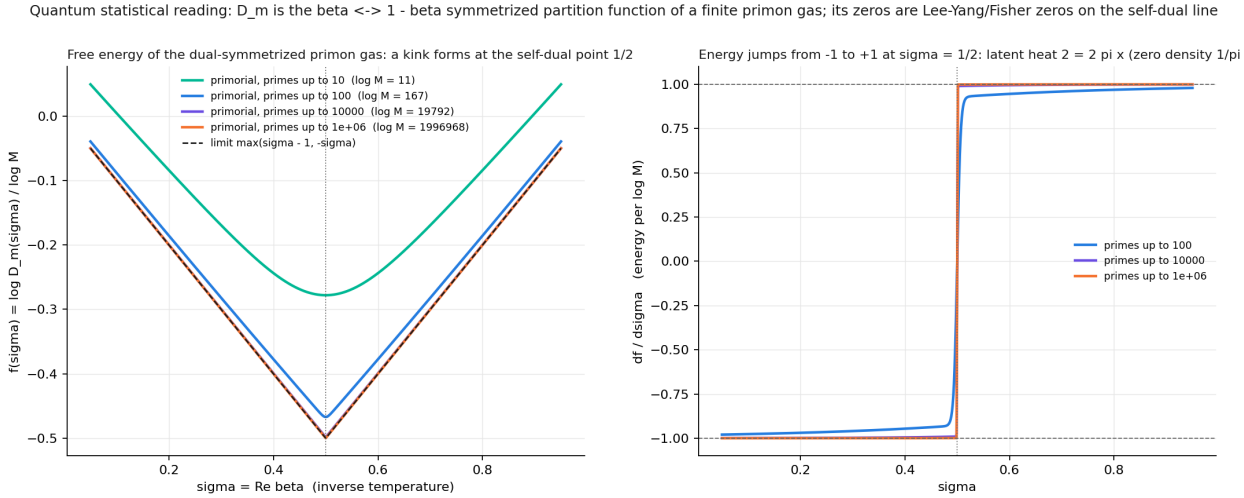

FIGURE 10. Free energy $\log D_m(\sigma)/\log M$ of the symmetrized primon gas along primorials (left) and its derivative (right): a corner forms at the self-dual point $\sigma = \frac{1}{2}$, with jump 2.

13. SAMPLING: THE ZEROS AS A RIESZ BASIS OF EXPONENTIALS

On the line $D_m(\frac{1}{2} + iT) = 2M^{-1/2} \sum_{d|m} d^{-1/2} \cos\big(T \log(M/d)\big)$ is an exponential polynomial of type $\log M$ whose extreme frequencies $\pm \log M$ carry the nonzero coefficient $M^{-1/2}$, whose zeros

are real and simple, and whose gaps are bounded below (Corollary 11). It is therefore a sine-type function, and by the Levin–Golovin theorem [Lev] its zeros form a complete interpolating sequence for the Paley–Wiener space of type $\log M$.

Corollary 18 (arithmetic sampling)**.** *Let $\{\gamma_n\}_{n\in\mathbb{Z}}$ be the zeros of $D_m(\frac{1}{2}+iT)$. Then $\{e^{i\gamma_n x}\}$ is a Riesz basis of $L^2(-\log M, \log M)$, and every $f \in L^2(\mathbb{R})$ whose Fourier transform is supported in $[-\log M, \log M]$ satisfies*

$$f(T) = \sum_n f(\gamma_n)\, \frac{D_m(\frac{1}{2}+iT)}{D_m'(\gamma_n)\,(T-\gamma_n)}.$$

The normalized zeros $\gamma_n \log M/\pi$ deviate from the lattice $n-\frac{1}{2}$ by $S_m(\gamma_n)$. Kadec's $\frac{1}{4}$ theorem [Kad] guarantees a Riesz basis when the deviation stays below $\frac{1}{4}$, and $\frac{1}{4}$ is sharp. For $m=2$, $\sup|S_2| = \arcsin(2^{-1/2})/\pi = \frac{1}{4}$ exactly: D_2 sits on Kadec's threshold and still gives a Riesz basis, because it is sine-type. The Riesz bounds (extreme eigenvalues of the normalized Gram matrix of $e^{i\gamma_n x}$ on $(-\log M, \log M)$) are stable as the number of zeros grows: $[0.375, 1.772]$ for $m=2$, $[0.508, 1.596]$ for $m=3$, $[0.108, 1.780]$ for $m=6$, $[0.170, 1.766]$ for $m=10$, $[0.105, 1.755]$ for $m=12$, and about $[0.035, 1.773]$ for $m=30$. A random band-limited signal is recovered from 6000 samples at the zeros of D_{12} with maximal relative error $1.2\cdot 10^{-9}$ (Figure 11).

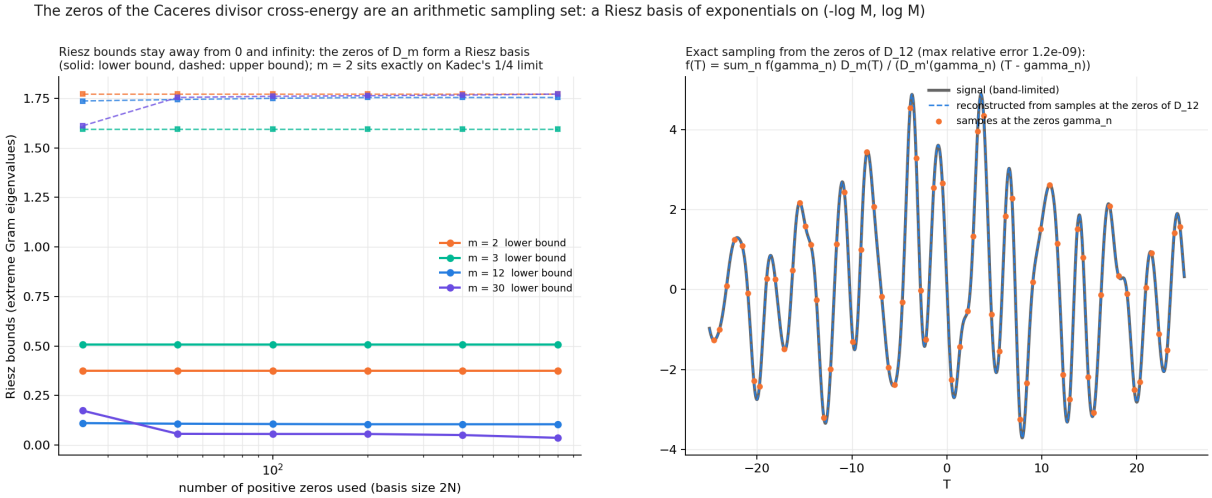

FIGURE 11. Left: Riesz bounds of $\{e^{i\gamma_n x}\}$ on $(-\log M, \log M)$ as the number of zeros grows (solid: lower, dashed: upper). Right: exact reconstruction of a band-limited signal from its samples at the zeros of D_{12}.

14. The bridge from divisors to sizes

The size cut and the divisor cut agree on $n<N$ when m is a multiple of $\operatorname{lcm}(1,\dots,N-1)$; the size cut is the divisor object with the large divisors removed and the scale M replaced by N.

Proposition 19. (1) *For $\sigma > \frac{1}{2}$ and $K_p \to \infty$, $E_m(1-s)/E_m(s) \to 0$, and $M^{1-s}E_m(s) = \prod_{p\mid m} \frac{1-p^{-K_p s}}{1-p^{-s}}$ is a truncated partial Euler product.*

(2) *For the size cut, $E_N(s) = \zeta(s)N^{s-1} + \frac{1}{1-s} + O(N^{-1})$; the arithmetic part $F(s) = \zeta(s)N^{s-1}$ has $F(1-s)/F(s) = N^{1-2s}\chi(1-s)$, whose modulus is <1 for $\sigma > \frac{1}{2}$ and $t < 2\pi N^2$ approximately. The Hermite–Biehler inequality $|F(s)| > |F(1-s)|$ fails exactly where $F(s)=0$, that is, at zeros of ζ.*

Hence a passage from Theorem 6 to the size cut which keeps the inequality amounts to partial Euler products representing ζ in $\frac{1}{2} < \sigma < 1$.

Proof. (1) $|E_p(1-s)/E_p(s)| = |R(1/w)|/|R(w)| \le |w|^{-K} \to 0$. (2) The functional equation gives $\zeta(1-s) = \chi(1-s)\zeta(s)$ identically, so the quotient is $N^{1-2s}\chi(1-s)$; its modulus is $(2\pi N^2/t)^{1/2-\sigma}$ up to $1 + O(1/t)$ by Stirling. □

For a nontrivial character, convergence of the Euler product of $L(s,\chi)$ in $\operatorname{Re} s > \frac{1}{2}$ is equivalent to the generalized Riemann hypothesis [Co, KKK]; for ζ the pole requires a modified product (the deep Riemann hypothesis). The divisor-to-size passage therefore lands on a known equivalence. A remark on any attempt to bridge the gap by a correction: if $\zeta = P_X \cdot C_X$ with a partial Euler product P_X, then C_X vanishes exactly at the zeros of ζ, since $P_X \neq 0$; and the functional equation fixes only $C_X(s)/C_X(1-s) = \chi(s)P_X(1-s)/P_X(s)$, which is blind to a pair of zeros $\rho, 1-\rho$, where both sides are $0/0$. Numerically $|\log(\zeta/P_X)|$ at $0.52+14.13i$ is $2.04, 1.48, 0.65, 1.42$ for $X = 10^2, \dots, 10^5$, and $|\log P_X(s)P_X(1-s) - \log\zeta(s)\zeta(1-s)|$ at $0.75+20i$ grows from 0.76 to 114.8 between $X = 10^2$ and 10^6, because $1-s$ lies in the left half of the strip. The hybrid product of [GHK] supplies C_X as a product over the zeros.

15. The λ-ladder

The function $\widehat{\Xi}(\lambda) = \xi(s)$, $\lambda = s(1-s)$, is entire of order $\frac{1}{2}$ in λ, with zeros λ_ρ, one for each pair $\{\rho, 1-\rho\}$, and $\widehat{\Xi}(\lambda)/\widehat{\Xi}(0) = \prod_\rho (1 - \lambda/\lambda_\rho)$. Its Taylor coefficients at $\lambda = 0$ give, by Newton's identities, the power sums

$$\sigma_k = \sum_\rho \lambda_\rho^{-k} \qquad (k \ge 1),$$

without using any zero; $\sigma_1 = \frac{1}{2}(2 + \gamma_E - \log 4\pi) = 0.0230957089661210338\ldots$ (checked to 20 digits). These are values of the zeta function over the zeros studied by Voros [Vo].

Proposition 20 (Ladder)**.** *Let $\lambda_1 \le \lambda_2 \le \cdots$ be the λ_ρ and $R_k^{(n)} = \sigma_k - \sum_{j \le n} \lambda_j^{-k}$. If λ_j is real for every $j > n$, then for every $k \ge 1$*

$$\big(R_k^{(n)}\big)^{-1/k} \le \lambda_{n+1} \le R_k^{(n)}/R_{k+1}^{(n)},$$

and both bounds converge to λ_{n+1} as $k \to \infty$. An off-line pair with $\lambda = |\lambda|e^{i\theta}$, $\theta \approx (2\beta-1)/\gamma$, contributes $2|\lambda|^{-k}\cos k\theta$, which changes sign near $k \approx \pi\gamma/(2(2\beta-1))$, where the bracket fails.

Proof. $R_k^{(n)} = \sum_{j>n} \lambda_j^{-k}$ is the k-th moment of a positive measure on $(0, \lambda_{n+1}^{-1}]$. It is at least λ_{n+1}^{-k}, which gives the lower bound; R_{k+1}/R_k is a weighted mean of the λ_j^{-1}, at most λ_{n+1}^{-1}, which gives the upper bound; it increases with k by Cauchy–Schwarz and tends to the largest atom. □

By the crossing law $\lambda_\rho = N_\rho^* - \frac{1}{12} - \frac{1}{180\lambda_\rho}$, Table 7 is the ladder of the crossing points of C_2^{FR}: each new crossing is fixed, up to the bracket, by the previous ones. The Riemann hypothesis is equivalent to the residues $R_k^{(n)}$ being Stieltjes moment sequences for all k; a finite ladder excludes only zeros with $\beta - \frac{1}{2} \gtrsim \gamma/k$.

16. The harmonic-function criterion revisited

Part V of [Ca17] uses the exact identity, valid for every real β,

$$|X(\tfrac{1}{2} + i\beta, n)|^2 = H_n + \sum_{k=1}^{n} \sum_{j \ne k} (kj)^{-1/2} \cos\Big(\beta \log \frac{k}{j}\Big), \qquad H_n = \sum_{k \le n} \frac{1}{k}, \tag{7}$$

and states that at a zero $H_n - O(n) - P(n) \to 0$, with $O(n) = n/(\beta^2 + \frac{1}{4})$ and $P(n)$ the double sum with a minus sign.

TABLE 7. The ladder with $k = 23$: each zero bracketed from the constants σ_k and the previous zeros (computed at 80 digits; Taylor coefficients by a Cauchy integral on $|\lambda| = 120$).

n	lower bound	upper bound	true λ_{n+1}	bracket for γ_{n+1}
0	200.040455	200.040456	200.040455	$[14.1347, 14.1347]$
1	442.1696	442.2202	442.1762	$[21.0219, 21.0231]$
2	625.7896	625.8186	625.7930	$[25.0108, 25.0114]$
3	924.884	929.408	925.923	$[30.408, 30.482]$
4	1084.858	1085.565	1084.968	$[32.933, 32.944]$
5	1411.66	1417.83	1412.97	$[37.569, 37.651]$
6	1669.48	1687.18	1674.59	$[40.856, 41.072]$
7	1876.61	1881.40	1877.49	$[43.317, 43.372]$
8	2286.48	2334.56	2304.74	$[47.81, 48.31]$
9	2471.36	2495.31	2477.68	$[49.71, 49.95]$

Proposition 21. *At a zero $\frac{1}{2} + i\beta$,*

$$H_n - O(n) - P(n) = |X_n|^2 - \frac{n}{\lambda} \longrightarrow \frac{1}{2\lambda}, \qquad \lambda = \tfrac{1}{4} + \beta^2.$$

Consequently the comparison between two zeros in [Ca17, (24)] *must be made with $H(\beta, n) + \frac{1}{2\lambda_\beta}$.*

Proof. Proposition 3. Numerically $|X_n|^2 - n/\lambda = 0.002500$ at $n = 10^5, 10^6$ for γ_1 against $\frac{1}{2\lambda} = 0.002499$, and 0.001131 for γ_2 against 0.001131. □

TABLE 8. Algorithm H2 of [Ca17] from the known zero $\beta_1 = 14.134725142$: roots of $H(\beta, n) - H(\beta_1, n)$ (original) and of the corrected comparison.

	$n = 60$ original	$n = 60$ corrected	$n = 400$ corrected	true
β_3	25.0083	25.0109	25.0109	25.010858
β_4	30.4356	30.4248	30.4249	30.424876

Spurious matches at non-zeros remain at finite n (for instance 25.38 and 30.39 at $n = 60$). Off the line, the object that carries the law is $X_n(s)X_n(1-s)$, not $|X_n|^2$. With $x = \alpha - \frac{1}{2}$ and $L = \log(j/k)$,

$$X_n(s)X_n(1-s) = H_n + \sum_{j \neq k} (jk)^{-1/2} \Big(\cosh(xL)\cos(\beta L) + i \sinh(xL)\sin(\beta L) \Big).$$

Proposition 22 (The oscillation is ζ)**.** *For $0 < \sigma < 1$, $s \neq \frac{1}{2} + i\beta$ with $\zeta(1-s) \neq \infty$,*

$$X_n(s)X_n(1-s) = \frac{n}{\lambda_s} + \frac{1}{2\lambda_s} + \zeta(s)\frac{n^s}{s} + \zeta(1-s)\frac{n^{1-s}}{1-s} + \zeta(s)\zeta(1-s) + o(1).$$

For $\sigma > \frac{1}{2}$ the term $\zeta(s)n^s/s$ is the oscillation of order n^σ; it vanishes exactly when $\zeta(s) = 0$.

Proof. Multiply the Euler–Maclaurin expansions at s and $1 - s$. Numerically, at $s = 0.7 + 20i$ the residual divided by n^s/s is $0.55728 - 0.88299i$ at $n = 10^6$, against $\zeta(s) = 0.55727 - 0.88300i$. □

So the statement that the $\sinh \cdot \sin$ sum keeps its n^σ oscillation off the line is, word for word, $\zeta(s) \neq 0$ for $\sigma > \frac{1}{2}$. In [Ca17, Part IV] the step "$|X|^2$ is a straight line if and only if $\operatorname{Re} z = \frac{1}{2}$" uses $|X|^2$, which is the right object only on the line.

17. The cross-energy of the primes

For the partial Euler product, $\log P_X(s)P_X(1-s) = \sum_{p\le X}\left(p^{-s}+p^{s-1}\right)+\cdots$, and

$$p^{-s}+p^{s-1} = 2p^{-1/2}\cosh\left((s-\tfrac12)\log p\right).$$

This is (3) with frequencies $\log p$ in place of $\log(N/k)$: a cross-energy of the primes. With the prime zeta function $P(s) = \sum_p p^{-s} = \sum_{k\ge1}\frac{\mu(k)}{k}\log\zeta(ks)$ [LW], let $F(s) = P(s)+P(1-s)$. Möbius inversion gives

$$\log\zeta(s)+\log\zeta(1-s) = F(s) - \sum_{k\ge2}\frac{\mu(k)}{k}\Big(\log\zeta(ks)+\log\zeta(k(1-s))\Big) \pmod{2\pi i}, \tag{8}$$

checked numerically to $5.8\cdot10^{-8}$ at $0.7+20i$ and $8.7\cdot10^{-10}$ at $0.6+7.3i$ with 60 terms. In the strip $P(s)$ is defined by this continuation; $\sum_{p\le X}p^{-s}$ does not converge there unconditionally.

Proposition 23 (Ladder of singular lines)**.** *In $0<\sigma<1$, $t\neq0$, the singularities of F are the points ρ/k and $1-\rho/k$, k squarefree, ρ a zero of ζ. Under RH they lie on the lines $\operatorname{Re}s=\frac12$ and $\operatorname{Re}s=\frac{1}{2k},1-\frac{1}{2k}$ ($k\ge2$ squarefree). In the band $\frac12<\sigma<\frac34$,*

$$F(s) = 2\log\zeta(s) - \log\chi(s) - \tfrac12\log\zeta(2-2s) - \tfrac13\log\zeta(3-3s) + R(s), \tag{9}$$

with $R(s) = \sum_{k\ge2}\frac{\mu(k)}{k}\log\zeta(ks) + \sum_{k\ge5}\frac{\mu(k)}{k}\log\zeta(k(1-s))$ absolutely convergent. A zero $\beta+i\gamma$ with $\beta>\frac12$ produces a singularity of F at $1-\rho/2$, with real part $1-\beta/2\in(\frac12,\frac34)$; hence, barring exact cancellation of multiplicities, RH holds if and only if F is holomorphic in $\frac12<\sigma<\frac34$, $t\neq0$.

Proof. $\log\zeta(ks)$ is singular exactly at $ks\in\{\rho,1\}$, and $\log\zeta(k(1-s))$ at $k(1-s)\in\{\rho,1\}$. For $\sigma>\frac12$ and $k\ge2$, $\operatorname{Re}ks>1$; for $k\ge5$ and $\sigma<\frac34$, $\operatorname{Re}k(1-s)>1$. The term $k=1$ of $P(1-s)$ is $\log\zeta(1-s) = \log\zeta(s)-\log\chi(s)$, and $\mu(2)=\mu(3)=-1$. The only singularity of the active terms in the band under RH is the pole of $\zeta(3-3s)$ at $s=\frac23$, on the real axis. □

The equivalence is immediate: holomorphy of F in the band is the absence of zeros of $\zeta(2-2s)$ there. What (9) adds is the coupling: the map $s\mapsto2-2s$ sends the thin band $(\frac12,\frac34)$ onto the whole right half $(\frac12,1)$, a hypothetical zero at β reappears at distance $\frac{1-\beta}{2}$ from the line, and the iteration $s\mapsto1-\frac{s}{2}$ has its fixed point at $\frac23$, the pole of $\zeta(3-3s)$. Since (8) is an identity valid for every configuration of zeros, it cannot by itself exclude any; it would become a constraint only with an independent analytic description of $\sum_p p^{-s}$ in the strip.

18. What C_2^{FR} can decide analytically

18.1. Factorization.

Lemma 24 (Factorization)**.** *For $0<\sigma<1$ and $N\ge2$, with $H_N(s) = N^{s-1}+\chi(1-s)N^{-s}$,*

$$T_N(s) := C_2^{\mathrm{FR}}(N,s) - \Big[\frac{1}{\lambda_s} - \frac{1}{N} - \frac{1}{12N^2} + \frac{2-3\lambda_s}{240N^4}\Big] = \zeta(s)H_N(s) + O\big((1+|s|)^5N^{-6}\big).$$

H_N has no zeros in $\sigma>\frac12$ for $t<2\pi N^2$ approximately, and $R_X=\zeta/P_X$, with P_X a partial Euler product that never vanishes. Hence, in such a region, the arithmetic part of C_2^{FR}, the rough zeta function R_X and ζ vanish at the same points.

Proof. Insert $\zeta(1-s)=\chi(1-s)\zeta(s)$ into (2); the size of H_N is Proposition 19(2). □

The left side of the first identity is a finite sum and explicit terms, without ζ. Any lower bound for it in $\sigma>\frac12$ is a lower bound for $|\zeta(s)H_N(s)|$; neither C_2^{FR} nor R_X contains information on $|\zeta|$ beyond ζ itself.

18.2. **A Turán-type criterion.**

Proposition 25. *$T_N(s)/H_N(s) \to \zeta(s)$ uniformly on every compact $K \subset \{\frac{1}{2} < \sigma < 1,\ t > 0\}$. Consequently the Riemann hypothesis holds if and only if, for every such K, T_N has no zeros on K for all $N \geq N_0(K)$.*

Proof. Uniform convergence is Lemma 24. If $T_N \neq 0$ on K for large N, Hurwitz's theorem gives $\zeta \neq 0$ on K (as $\zeta \not\equiv 0$). Conversely, if $\zeta \neq 0$ on K, $|\zeta H_N|$ is bounded below on K for large N and the error tends to 0. □

Turán proposed the analogous criterion for the partial sums X_N; it fails because X_N has zeros in $\sigma > 1$ for large N [Mo]. The sum T_N behaves differently. Its zeros with $\sigma > \frac{1}{2}$ (search on $0.502 \leq \sigma \leq 1$):

N	10	20	50	100
zeros, $\sigma > \frac{1}{2}$, $2 < t < 60$	1	0	0	0
first one at	$0.562 + 43.37i$	$0.514 + 67.09i$	$0.562 + 266.60i$	$0.519 + 559.35i$

For comparison, X_{19} has 12 zeros with $\sigma > \frac{1}{2}$ and $t < 60$. The frontier $t^*(N) \approx 3$–$6N$ is set by the truncation of the Euler–Maclaurin terms, not by ζ. On the line T_N has many more sign changes than ζ ($55, 73, 85$ for $N = 20, 50, 100$ and $2 < t < 60$, against 10): they are the zeros of H_N.

18.3. **The nodal count of C_2.** The cross-energy $C_2(N,s) = |X_N|^2 - |X_{N-1}|^2 - N^{-2\sigma} = 2N^{-\sigma}\sum_{n<N} n^{-\sigma}\cos(t\log\frac{N}{n})$ is real and not holomorphic; its zeros are curves. Write $C_2 = 2N^{1-2\sigma}(1-\sigma)/|1-s|^2 + 2\,\mathrm{Re}\,\big(A_N(s)N^{-\bar{s}}\big)$ with $A_N(s) = X_{N-1}(s) - N^{1-s}/(1-s)$. Where the wave dominates, the number of sign changes on a vertical segment $T_0 < t < T_1$ is $\big((T_1-T_0)\log N + \Delta_t \arg A_N\big)/\pi$, so by the argument principle it changes by 2 each time σ crosses a zero of A_N. With $N = 2000$ and $10 < t < 60$ (full count 121), the count is 121 for every $\sigma \in [0.52, 1.20]$ with the coefficients of ζ. With the Epstein coefficients of Section 6 it falls in steps of 2 ($121, 119, 117, 115, 113, 111, 109, 105$ at $\sigma = 0.94, 0.92, 0.88, 0.80, 0.78, 0.72, 0.64, 0.56$) as σ crosses its zeros $0.938 + 29.98i$, $0.933 + 15.67i$, $0.823 + 44.00i$, $0.811 + 58.51i$, $0.635 + 46.76i$, $0.597 + 52.74i$ (Figure 12; at finite N the steps are shifted, and the step at 0.72 matches none of these zeros). This reads RH as the constancy in $\sigma > \frac{1}{2}$ of the number of sign changes of real cosine sums.

18.4. **The weighted trapezoid form.** Summing the trapezoid errors of x^{-s} on the arcs $[k, k+1]$, whose weight is $P(x) = \{x\}(1-\{x\}) \geq 0$, gives an exact form of the collapse at the zeros.

Proposition 26. *For $0 < \sigma < 1$,*

$$\zeta(s) = \tfrac{1}{2}s(s+1)\Big(J(s) - \frac{1}{\lambda_s}\Big), \qquad J(s) = \int_1^\infty \{x\}(1-\{x\})\, x^{-s-2}\, dx.$$

Hence $\zeta(s) = 0$ if and only if $J(s) = 1/\lambda_s$. Moreover $|J(s)| \leq J(\sigma) \leq \frac{1}{4(1+\sigma)}$, so there is no zero on $(0,1)$, where $1/\lambda_\sigma \geq 4$, and none with $|s(1-s)| < 4(1+\sigma)$.

Proof. For $\sigma > 1$, the trapezoid rule on $[k, k+1]$ gives $\frac{f(k)+f(k+1)}{2} - \int_k^{k+1} f = \frac{1}{2}\int_k^{k+1} Pf''$; with $f(x) = x^{-s}$ and summation over $k \geq 1$, $\zeta(s) = \frac{1}{s-1} + \frac{1}{2} + \frac{s(s+1)}{2}J(s)$, and both sides continue to $\sigma > -1$. Since $\frac{1}{s-1} + \frac{1}{2} = \frac{s+1}{2(s-1)} = -\frac{s(s+1)}{2}\cdot\frac{1}{\lambda_s}$, the identity follows. The bounds use $0 \leq P \leq \frac{1}{4}$. Numerically $|J(\rho) - 1/\lambda_\rho| = 1.4\cdot 10^{-17}$ and $2.0\cdot 10^{-17}$ at the first two zeros. □

J is the Mellin transform of a positive weight, and the condition $J = 1/\lambda$ is the λ-collapse of C_2^{FR} in integral form. Splitting J at x_0, the tail $\int_{x_0}^\infty$ is of size $\lesssim x_0^{-\sigma-1}/(6t)$, negligible against $|1/\lambda| \approx t^{-2}$ once $x_0 \gtrsim t^{2/3}$; there the arcs are long and the trapezoid errors are controlled. The

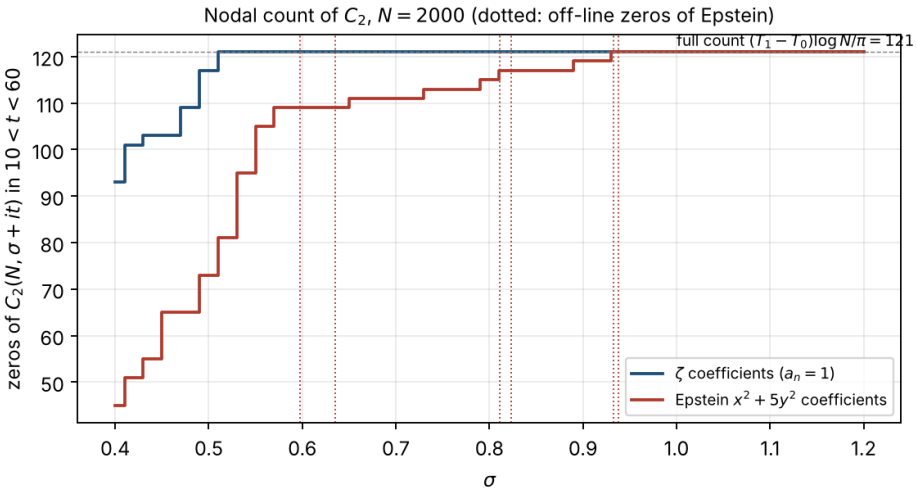

FIGURE 12. Number of zeros of $C_2(N, \sigma + it)$ in $10 < t < 60$ as a function of σ, $N = 2000$. Coefficients of ζ (blue) and of the Epstein function of $x^2 + 5y^2$ (red; dotted lines at its off-line zeros).

head $\int_1^{x_0}$, $x_0 \approx t^{2/3}$, contains the arcs on which $\cos(t \log x)$ oscillates faster than the integer grid. Convexity gives no sign there, and the whole question is whether this finite oscillatory integral can take the value $1/\lambda_s$ minus the tail when $\sigma > \frac{1}{2}$.

19. Discussion

The Caceres divisor cross-energy is the smallest object with an Euler product and the symmetry $s \leftrightarrow 1 - s$ in which everything can be computed. All its properties come from one fact: E_m is a product of local factors, one for each prime, and each factor is stable, its Blaschke product β_p having its zeros at the roots of unity scaled by $p^{-1/2}$. From this follow the zeros on the line ($|B_m| < 1$ off it), the monotone phase and the exact counting (a sum of Poisson kernels), the quasicrystal and its extinction rule (B_m^{-1} is analytic on a torus with one axis for each prime), the exact supremum and the interlacing threshold (the primes act independently, by Kronecker), the classification (a single unstable prime cannot be compensated), the quantum graph (a unitary realization of $\prod_p \beta_p$) and the sampling property (a sine-type function). The general frames are known — stable polynomials and crystalline measures [KS, ACV], quantum graphs [GS], Lee–Yang theory [LY], sine-type functions [Lev] — and D_m is an explicit arithmetic family inside them, indexed by the integers, with exact constants.

The results of this paper locate the difficulty in one place. The reflected cross-energy is a Hermite–Biehler pair $E_N(s) + E_N(1 - s)$ whose inequality fails at the zeros of ζ and nowhere else (Proposition 19); its zeros off the line are transient for ζ and permanent for the two controls (Section 3). The Epstein control shows that pole, functional equation, positivity and the translation law do not decide (Corollary 4). The Euler product does decide at every finite stage when the Dirichlet sum is cut by divisors (Theorem 6), and the passage to the cut by size is the convergence of partial Euler products in the strip, an equivalent of the Riemann hypothesis. The ladder (Proposition 20) and the correction of [Ca17] (Proposition 21) are tools that compute the zeros on the line from earlier data; Proposition 22 and Proposition 23 show that the off-line content of these formulas is exactly $\zeta(s) \neq 0$. We do not prove the Riemann hypothesis.

20. Open notes

(1) *Interpolating cuts.* Find weights $w(n)$ interpolating between the divisor cut and the size cut for which $|E(s)| > |E(1-s)|$ persists for $\sigma > \frac{1}{2}$; product weights $\prod_p w_p(v_p(n))$ with $w_p(k+1) \le \sqrt{p}\, w_p(k)$ keep Theorem 6, size cuts do not.

(2) *The $1/\sqrt{N}$ law.* Prove that, if all zeros of ζ below T are simple and on the line, every zero of $C_2^{\mathrm{FR}}(N,\cdot)$ with $t \le T$ satisfies $|\sigma - \frac{1}{2}| \le K(T)/\sqrt{N}$ for large N, and compute $K(T)$ from $|\zeta'(\rho)|$ and the collision geometry of Proposition 2.

(3) *Genealogy of the Epstein zeros.* Trace back in N the permanent off-line zeros of the Epstein C_2^{FR} and find whether they are born from a collision on the line or enter from large σ.

(4) *Larger ladders.* Push Table 7 to $k = 200$ with 300-digit arithmetic and measure how the bracket width scales with n and k.

Data and code

Python scripts (NumPy, mpmath, Matplotlib) in the ancillary file: `gen.py` (genealogy of the zeros of C_2^{FR} for ζ and the Davenport–Heilbronn coefficients, Table 1); `fam.py` (Table 2); `epstein.py` (Table 3); `ep_gen.py` (Table 4 and the Epstein C_2^{FR}); `mult.py` (Theorem 6, numerical comparison); `ladder.py` (Table 7); `plot_divisor_cross_energy.py` and `zeros_divisor_cross_energy.py` (Figures 2–4, Table 6); `step1_counting_quasicrystal.py` (Theorem 10, Figure 5); `step2_diffraction_closed_form.py` and `step2_figure.py` (Theorem 13, Figure 6); `step3_interlacing.py` and `step3_density.py` (Section 10); `step4_classification.py` and `step4_figure.py` (Figure 8); `step5_operator.py` and `step5_figure.py` (Theorem 17); `step6_primon_gas.py` (Figure 10); `step7_riesz_sampling.py` (Figure 11); the remaining checks are short scripts recorded in `NOTES_C2FR_genealogy.md` and `NOTES_divisor_cross_energy.md`.

Use of AI assistance

The cross-energy and the research programme of this series are the author's. Claude (Anthropic) was used as a research and writing aid: to derive and check proofs, to write and run the Python computations, to test statements against controls, to search the literature, and to draft and edit text and figures. The author checked all results and is responsible for the content.

References

[ACV] L. Alon, A. Cohen, C. Vinzant, Every real-rooted exponential polynomial is the restriction of a Lee–Yang polynomial, preprint, arXiv:2303.03201, 2023.

[Cl] D. N. Clark, One dimensional perturbations of restricted shifts, *J. Analyse Math.* 25 (1972), 169–191.

[Co] K. Conrad, Partial Euler products on the critical line, *Canad. J. Math.* 57 (2005), 267–297.

[DH] H. Davenport, H. Heilbronn, On the zeros of certain Dirichlet series I, II, *J. London Math. Soc.* 11 (1936), 181–185, 307–312.

[EW] P. Erdős, A. Wintner, Additive arithmetical functions and statistical independence, *Amer. J. Math.* 61 (1939), 713–721.

[GS] S. Gnutzmann, U. Smilansky, Quantum graphs: applications to quantum chaos and universal spectral statistics, *Adv. Phys.* 55 (2006), 527–625.

[GHK] S. M. Gonek, C. P. Hughes, J. P. Keating, A hybrid Euler–Hadamard product for the Riemann zeta function, *Duke Math. J.* 136 (2007), 507–549.

[JT] B. Jessen, H. Tornehave, Mean motions and zeros of almost periodic functions, *Acta Math.* 77 (1945), 137–279.

[Ju] B. Julia, Statistical theory of numbers, in *Number Theory and Physics*, Springer Proc. Phys. 47, 1990, 276–293.

[Ka] S. Kakeya, On the limits of the roots of an algebraic equation with positive coefficients, *Tôhoku Math. J.* 2 (1912), 140–142.

[Kad] M. I. Kadec, The exact value of the Paley–Wiener constant, *Soviet Math. Dokl.* 5 (1964), 559–561.

[KKK] T. Kimura, S. Koyama, N. Kurokawa, Euler products beyond the boundary, *Lett. Math. Phys.* 104 (2014), 1–19.

[KS] P. Kurasov, P. Sarnak, Stable polynomials and crystalline measures, *J. Math. Phys.* 61 (2020), 083501; arXiv:2004.05678.
[Le] B. Ja. Levin, *Distribution of Zeros of Entire Functions*, Transl. Math. Monographs 5, AMS, 1964.
[Lev] B. Ya. Levin, *Lectures on Entire Functions*, Transl. Math. Monographs 150, AMS, 1996.
[LY] T. D. Lee, C. N. Yang, Statistical theory of equations of state and phase transitions II. Lattice gas and Ising model, *Phys. Rev.* 87 (1952), 410–419.
[LW] E. Landau, A. Walfisz, Über die Nichtfortsetzbarkeit einiger durch Dirichletsche Reihen definierter Funktionen, *Rend. Circ. Mat. Palermo* 44 (1920), 82–86.
[Mo] H. L. Montgomery, Zeros of approximations to the zeta function, in *Studies in Pure Mathematics*, Birkhäuser, 1983, 497–506.
[Po] G. Pólya, Über die Nullstellen gewisser ganzer Funktionen, *Math. Z.* **2** (1918), 352–383.
[PS] G. Pólya, G. Szegő, *Problems and Theorems in Analysis I*, Springer, 1972.
[Vo] A. Voros, *Zeta Functions over Zeros of Zeta Functions*, Lecture Notes of the UMI 8, Springer, 2010.
[Ca17] P. Caceres, Proof of the Riemann hypothesis using the decomposition $\zeta(z) = X(z) - Y(z)$, manuscript, 2017–2024.
[CE0] P. Caceres, An overview of the series, preprint, 2026.
[CE13] P. Caceres, The Euler cross-energy, Weil positivity and a one-variable form of the Riemann hypothesis, preprint, 2026.
[CE21] P. Caceres, The minimizer of the Weil form in a window, and the scale $2\pi N$, preprint, 2026.
[CE32] P. Caceres, The reflected cross-energy at the critical line, preprint, 2026.
[CE41] P. Caceres, Structural limits of the cross-energy method, preprint, 2026.
[CE42] P. Caceres, Square roots of Weil's form: operators, Landau's test and the spectrum of the primes, preprint, 2026.
[CE46] P. Caceres, Controls for the Riemann hypothesis: Davenport–Heilbronn, Beurling systems and function fields, preprint, 2026.

Universidad Europea de Valencia, Valencia, Spain
Email address: pedrojesus.caceres@universidadeuropea.es
URL: https://orcid.org/0000-0002-6540-8993